rijksuniversiteit groningen

Bachelorthesis of Teun Zijp

Exploring the limits of CG-martini 3

Exploring the limits of CG-martini 3

Self-assembly of Hexa-peri-hexabenzocoronene, a Graphitic Nanotube

Teun Zijp, s2795795

October 13, 2017

Contents

Abstract: At the end of 2017, a new version of CG Martini will be released: Martini 3.0. Before it is released, it needs to be tested extensively.

During this bachelor-research, a Martini-model of Hexa-peri-hexabenzocoronene (HPHC) was built, validated, and the self-assembly process of HPHC was simulated. The hypothesis was that HPHC self-assembles into a tubular vesicle. Loose HPHC molecules successfully self-assembled into a nanowire, in which the $\pi - \pi$-stacking-distance is consistent with literature. Multiple nanowires successfully self-assembled into nanowire aggregates, e.g. a dimer and a tetramer. A membrane built out of HPHC molecules is stable, and membrane bending has been proven to be possible. Although the double-walled nanotube did not form yet, the results look promising.

1   Background

1.1   Molecular dynamics

Molecular Dynamics (MD) is one of the most common tools in computational biology. There are many software packages and force fields available.

In molecular dynamics, a force field describes the method how the potential energy of a system of particles is calculated. This potential energy contains both bonded and non-bonded interactions. The derivative of the potential energy with respect to a spatial coordinate is the force, in equation: $F(x) = -\frac{\partial E_{\text{pot}}}{\partial x}$. This force is then used to calculate the acceleration of atoms or coarse grained particles.

There are many force field. Each force field makes a different trade-off between speed and accuracy. E.g. CHARMM (1983), considers all atoms, but this becomes rather slow for big systems. For many simulations, like self-assembly of membranes, it is not necessary to have explicit hydrogens. They can be added implicitly by uniting them with heavy atoms, i.e. CH_2 is modeled as one particle. Because united atom models have fewer particles than all atom models, the computational effort is decreased, and therefore, the simulation speed is higher. There are multiple united atom force fields, e.g. Berger et al (see Figure 1.1), but also GROMOS (1987, 1996)[HLG11], and many others.

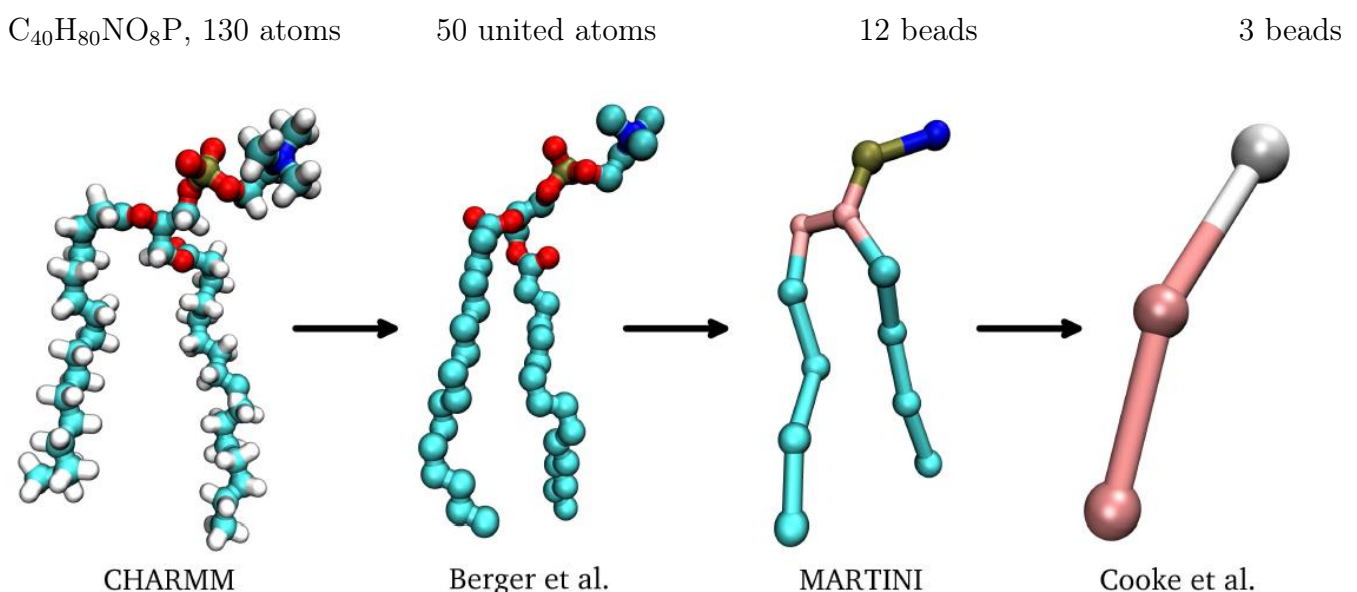| $C_{40}H_{80}NO_8P$, 130 atoms	50 united atoms	12 beads	3 beads

Figure 1.1: Four different models for the phospholipid DPPC, from all-atom to massively coarse-grained.
Image source: `http://2015.igem.org/Team:TU_Darmstadt/Project/Bio/Modeling/sec3`

More recently, coarse grained force fields are being developed, with most notably Martini (2004)[MVM04] and Cooke (2005). Cooke's force field is solvent-free, and only contains 2 types of particles: polar and apolar. The benefit of coarse grained modeling (coarse or graining) is that it is significantly faster than all or united atom. The disadvantage of coarse graining is that details are lost. Coarse graining to Cooke's level is only suitable for lipid bilayers, and even then, there is the problem that there is only one model that should represent all amphiphiles. Yet, the philosophy of coarse graining is clear: keep it simple.

1.2 The martini force field

In 2004, Siewert-Jan Marrink & Alex de Vries developed CG Martini; a coarse grained force field. The Martini philosophy is: each bead models 4 heavy atoms, there are 4 main types beads: polar (P), non-polar (N), apolar (C), and charged (Q). The non-bonded interactions are Lennard Jones-potentials, see Eq. 1.1, defined in a martini-file, which is validated by reproducing the octanol-water partitioning coefficient ($\log P_{\text{oct/wat}}$) of compounds found in literature[MVM04].

$$U_{LJ}(r) = 4\varepsilon_{ij}\left[\left(\frac{\sigma_{ij}}{r}\right)^{12} - \left(\frac{\sigma_{ij}}{r}\right)^6\right] \quad \text{(Eq. 1.1)} \qquad U_{el}(r) = \frac{q_i q_j}{4\pi\varepsilon_0\varepsilon_{\text{r}}r} \qquad \text{(Eq. 1.2)}$$
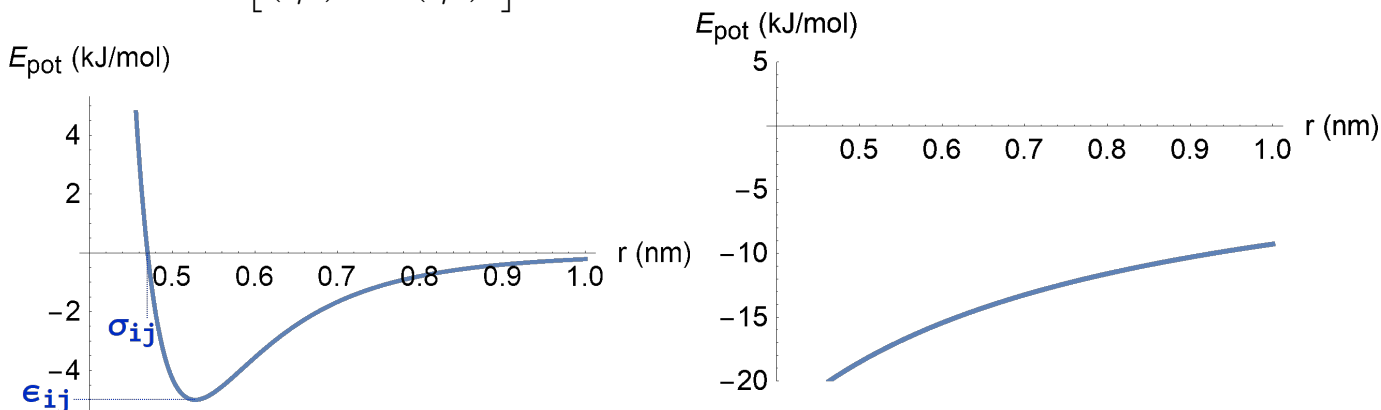
Figure 1.2: An example of a Lennard Jones potential. Here, the interaction between two C1 beads is shown ($\varepsilon_{ij} = 5$ kJ/mol, ($\sigma_{ij} = 0.47$ nm).

Figure 1.3: An example of a coulomb potential. Using $q_1 = -q_2 = 1e^-$. Note that for Coarse Grained Martini, $\varepsilon_{\text{r}} = 15$

Charged groups (type Q) have an electrostatic Coulombic potential, in addition to the Lennard-Jones potentials, see Eq. 1.2.

The name: why Martini?

"The name 'Martini' of the force field was coined in 2007 with the release of version 2.0. Martini is the nickname of the city of Groningen in the Netherlands where the force field was developed and where its development continues to date. A famous landmark in the city is the 100 m high Martini tower. The name also reflects the universality of the cocktail with the same name; how a few simple ingredients (chemical building blocks) can be endlessly varied to create a complex palette of taste." [PM13]

1.2.1 2004: Martini 1

In 2004, the first Martini-paper was published.

The flavors. There are subtypes for charged (Q) and non-polar (N)-beads: a letter denoted the hydrogen-bonding capabilities (d = donor, a = acceptor, da = both, 0 = none).

The levels. The interaction matrix was a 10×10 table, in which interactions range from attractive (level I, $\varepsilon = 5$ kJ/mol) to repulsive (level V, $\varepsilon = 1.8$ kJ/mol). For all five interaction types the same effective size is assumed, $\sigma_{ij} = 0.47$ nm. This relatively simple force field was specialized in modeling phospholipid membranes. [MVM04].

1.2.2   2007: Martini 2

In 2007, the second Martini-paper was published.

More flavors. This time, there are also subtypes for polar (P) and apolar (C) beads, which vary in their polar affinity from weak (1) to strong (5). For example: alkyl chains are modeled with C1 beads (superhydrophobic), and butadiene is modeled with C4 bead, because the π-cloud is polarizable and therefore has more polar affinity; propanol is modeled as P1, neutral acetic acid as P3, and four water molecules are modeled as one P4 bead.

More levels. `MARTINI 1` had only 5 interaction levels. In `MARTINI 2`, the interactions are now distinguished into 10 levels: from super attractive (level O, $\varepsilon = 5.6$ kJ/mol); attractive (level I, $\varepsilon = 5.0$ kJ/mol); to repulsive (level VIII, $\varepsilon = 2.0$ kJ/mol); and super repulsive (level IX, $\varepsilon = 2.0$ kJ/mol with σ_{ij} 0.62 nm). Note that $\sigma_{ij} = 0.47$ nm for all levels, except for level IX. Level IX is only used to model the interaction between a C1 or C2 bead and a Q-bead. [Mar+07].

Size matters. `MARTINI 2` also features small (S) beads, that allow 3:1 mapping. All beads can be scaled down by putting an S in front of the name, e.g. the C1 bead is a butane molecule (C_4H_{10}), while the the SC2 bead is a propane molecule (C_3H_8). Beads that do the 4:1 mapping will be referred to as normal beads, e.g. P4, which is the same P4 bead as the one of `MARTIN I 1`. This was implemented in order to allow the creation of rings: Cyclohexane is modeled by three SC1 beads, benzene by three SC3[1], see Figure 1.4. The interaction matrix for small beads (ring-ring-interactions) is scaled down to 75% of the original ε_{ij} values, and $\sigma = 0.43$ nm.

Future outlook. Martini 2 is great, but there is still room for improvement:

- P5 is a stable solid at room temperature, and P4 (water) has the tendency to freeze at room temperature too. There are anti-freeze particles available (BP4), which is implemented since Martini 2.0, but it would be better if water wouldn't freeze at room temperature.

- When Martini was used to model proteins, some problems occurred with charged groups in hydrophobic environments (interaction level IX is problematic). These problems were fixed by including some custom beads (AC1 and AC2 are added in Martini 2.1).

- A revision in 2012 lead to Martini 2.2p, a version that includes polarizable water. [MT13]

- In 2015, DNA was modeled with CG Martini, but it required custom beads.

- Mapping rings with small beads is good enough for benzene, but when modeling polyaromatic compounds, 3:1 mapping is too rough.

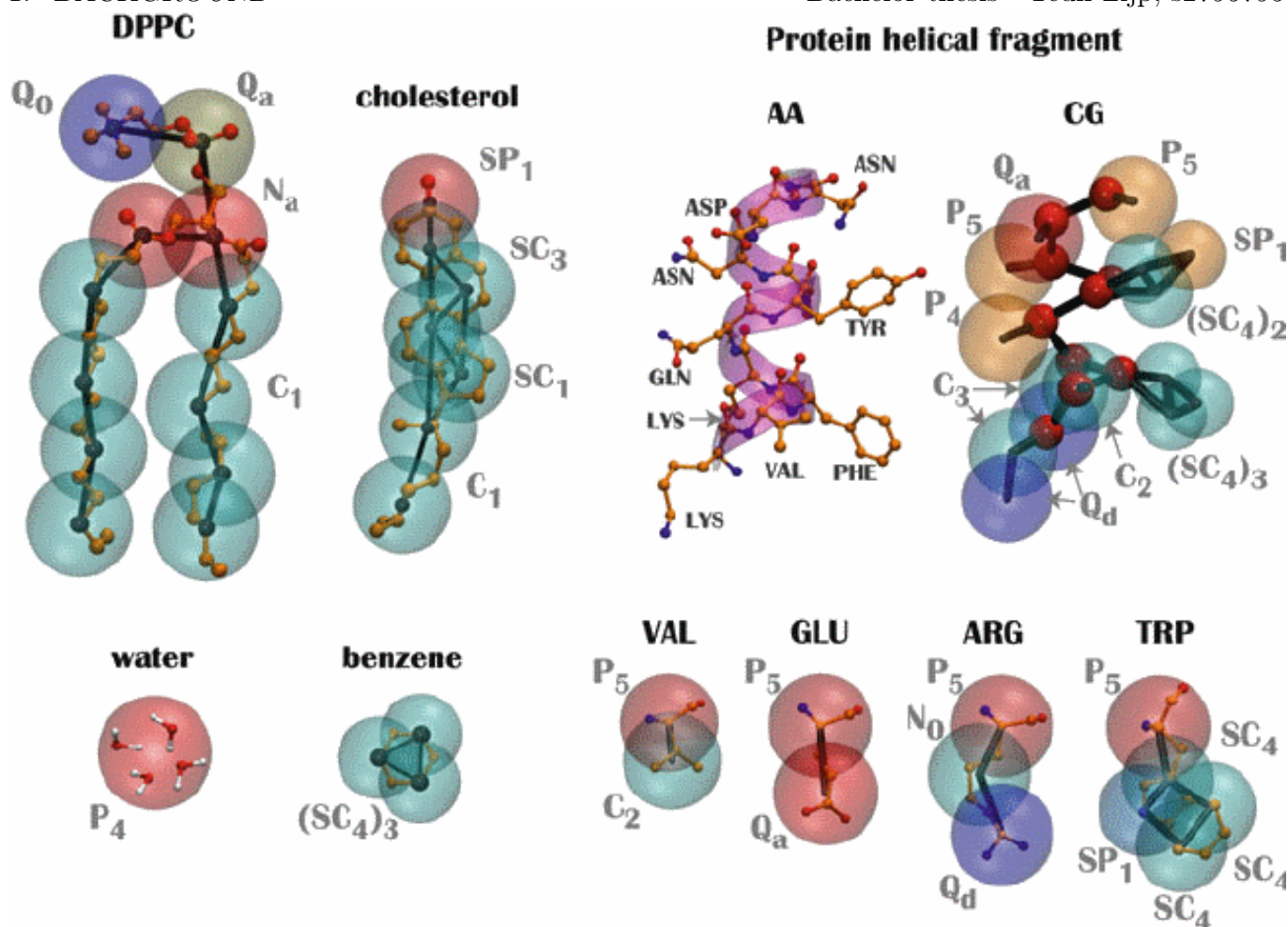[1]http://www.cgmartini.nl/images/parameters/ITP/martini_v2.0_solvents.itp

Figure 1.4: "The looks of Martini 2. Mapping between the chemical structure at the atomistic level (AA) with the coarse-grained (CG) Martini model for DPPC, cholesterol, water, benzene, a protein helical fragment, and a few amino acids (valine, glutamic acid, arginine, and tryptophan). The CG beads are shown as transparent vdW spheres. For clarity, in the case of the protein helical fragment the AA and CG representations are shown side-by-side and the CG backbone beads are represented by small spheres. Hydrogens are only shown for the atomistic water." [PM13]

1.2.3 Expected in 2017/2018: Martini 3

In 2016, the development of Martini 3 started, with the aim to improve accuracy. The interaction matrix will get more levels (17), so that the interaction matrix can be tuned better. This will allow to develop new water that does not freeze at room temperature. In order to model polyaromatic systems and other rings, tiny beads (T) are now also included, that do 2:1 mapping. This allows e.g. naphthalene to be mapped with tiny beads.

Paulo Telles de Souza is developing the next version of Martini; `MARTINI 3` *will be published soon.*

The beads in the beta-versions of Martini 3 are already validated with octanol/water partitioning for the key building blocks. Martini 3 will be tested more vigorously before it is released. Multiple sub-teams are set up, each team will test a specific purpose for Martini 3, e.g. DNA, proteins, and polyaromatic molecules.

In April 2017, I (Teun Zijp) joined the polyaromatic subteam of Martini 3. The next chapter introduces the topic of this research project in more detail.

2   Introduction: Amphiphilic Aggregates

Amphiphiles have both hydrophilic parts and hydrophobic tails. The hydrophobic tails avoid water-contact by forming interesting macroscopic shapes. Common examples are spheres (micelles, vesicles or liposomes), sheets (bilayers) and rods (e.g. nanowire aggregates and double-walled nanotubes).

The bilayer is the best known macromolecular structure for amphiphiles, mainly because cell-membranes are built out of phospholipid bilayers. Next, micelles are used to transport fatty molecules within the body, and vesicles are used to transport proteins and water-soluble molecules, see Figure 2.1a.
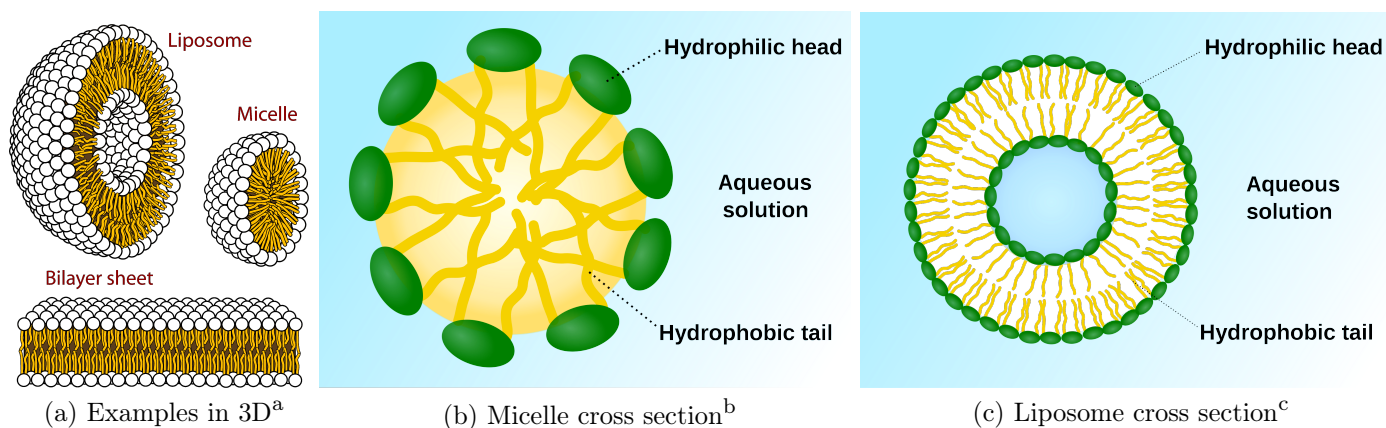

(a) Examples in 3D[a]   (b) Micelle cross section[b]   (c) Liposome cross section[c]

Figure 2.1: Various supramolecular shapes formed by amphiphiles. (a) Examples of supramolecular structures formed by amphiphiles in 3D[a]. (b) Cross-section of a micelle or nanowire aggregate[b]. (c) Cross-section of a liposome, vesicle or double-walled nanotube[c].

[a] Source: `https://commons.wikimedia.org/wiki/File:Phospholipids_aqueous_solution_structures.svg`
[b] Source: `https://commons.wikimedia.org/wiki/File:Micelle_scheme-en.svg`
[c] Source: `https://commons.wikimedia.org/wiki/File:Liposome_scheme-en.svg`

Note that both micelles and vesicles are spherical. Phospholipids do not form stable rod-like structures.

2.1   Rod-like amphiphilic structures: from Nanowires to Nanotubes

Rod-like supramolecular amphiphilic structures can be formed by a special type of amphiphiles: aromatic amphiphiles. The first step in the formation of rod-like structures is the formation of **"Nanowires"** that have the tendency to remain straight.

Nanowires. Aromatic molecules tend to stack on top of each other to form $\pi-$stacks. Long aggregated $\pi-$stacks will be referred to as "nanowires"[2]. If a few nanowires interact with other via the hydrophobic tails, they form a **nanowire aggregate**.

Nanowire aggregates. Nanowire aggregates have a cross section that is similar to that of a micelle, see Figure 2.1b. Nanowire aggregates can be named after the number of nanowires that formed this aggregate, e.g. dimer, trimer, tetramer, hexamer, etc. The nanowires can be entangled in a helical fashion, as shown in Figure 2.2d on the following page.

---

[2] ***Caution!*** Note that the general term "nanowire" in most cases refers to metallic needles. This is beyond the scope of this paper. All "nanowires" encountered here are actually long aggregated $\pi-$stacks.

Double-walled nanotubes. Double-walled nanotubes have a cross section that is similar to that of a liposome, see Figure 2.1c on the previous page. The nanowires can be straight, along the double walled nanotube, similar to the way nanowires are entangled in nanowire aggregates. The nanowires do not have to be straight, there are also other superstructures observed.

Mysterious Helical Super-structures. Every now and then, aromatic amphiphiles like to self-assemble into structures that have some sort of helical super-structure. For C_8O_3, the driving force for forming the helical super-structure has been found: it has to deal with non-straight π-stacking, as shown in Figure 2.2c. Charges in the aromatic system cause straight packing to be unfavourble.
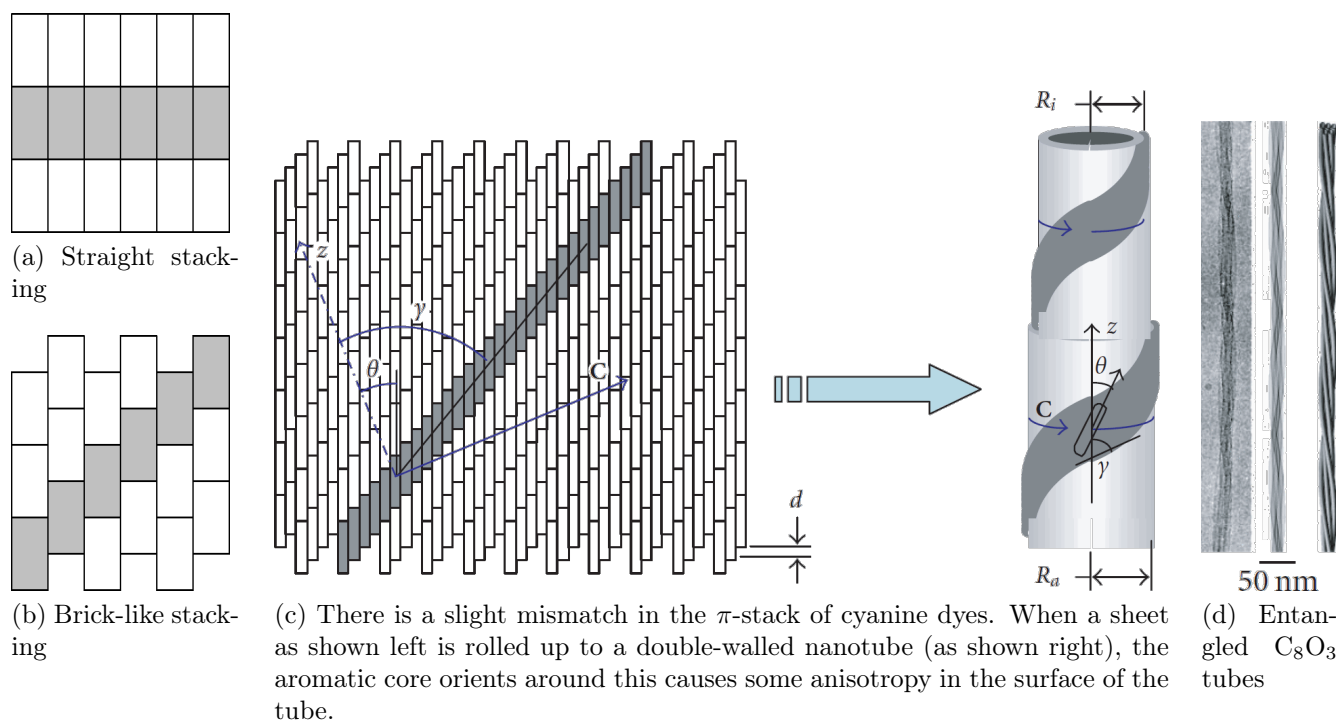

(a) Straight stacking

(b) Brick-like stacking

(c) There is a slight mismatch in the π-stack of cyanine dyes. When a sheet as shown left is rolled up to a double-walled nanotube (as shown right), the aromatic core orients around this causes some anisotropy in the surface of the tube.

(d) Entangled C_8O_3 tubes

Figure 2.2: Elaboration on the nanowire aggregation.
(a) If the aromatic cores of the molecules stack perfectly on top of each other, a straight π-stack is formed.
(b) If the aromatic core is charged, it is unfavourable to stack equal charges on top of each other. In the most extreme case, a brick-like π-stack could be formed.
(c) The aromatic core of cyanine dyes have a delocalized positive charge. This causes a slight offset in the stacking; this will be referred to as "diagonal stacking" or "chiral stacking". On the right, the position of the π-stack in the nanotube is emphasized in black. A double-walled nanotube like this will also be referred to as "a chiral tube".
(d) Due to the anisotropy of the nanotube surface, multiple tubes become entangled in a helical fashion.

Note that double-walled nanotubes can have mysterious helical super-structures too, e.g. hexa-peri-hexabenzocoronene (HPHC) self assembles into a double walled nanotube as shown in Figure 2.5 on page 12.

2.2 Cyanine dyes

Cyanine dyes are highly fluorescent, and can form J-aggregates or double-walled nanotubes, see Table 1. The asterisk (*) indicates that the morphology was confirmed by electron microscopy, in other cases, morphology was concluded from optical spectra. [KD06]

m	n	Trivial name	Morphology of aggregates
Carboxyl compounds (R = COOH)			
8	1	C8O1	no J-aggregates
8	2	C8O2	Tubular, chiral
8	3	C8O3*	
8	4	C8O4*	planar, achiral
2	3	C2O3	planar or linear, achiral
4	3	C4O3	
6	3	C6O3	
7	3	C7O3	
8	3	C8O3	
10	3	C10O3	tubular, chiral
11	3	C11O3	
12	3	C12O3	
Solfo-compounds (R = SO$_3$$^-$)			
8	2	C8S2*	ribbons/tubes
8	3	C8S3*	tubes (single)
2	3	C2S3 (BIC)	planar or linear
2	4	C2S4 (TDBC)	
4	4	C4S4	

Table 1: Names and morphologies of cyanine dyes. The asterisk (*) indicates that the morphology was confirmed by electron microscopy, in other cases, morphology was concluded from optical spectra.
Table taken from [KD06, p.4]

Figure 2.3: "5,5'6,6'-tetrachlorobenzimidacarbocyanine. The chemical variants this cyanide dye are identified by a mnemonic short phrase of the type **C$_m$R$_n$**, where m and n indicate the length of the alkyl chains at the 1,1'- and 3, 3'- positions, respectively. R is an abbreviation to denominate the ionic groups, O stands for R = COO$^-$ and S stands for R = SO$_3$$^-$. See also Table 1 for further information."
Image source: [KD06, p.3]

Note that Table 1 is not complete. The self-assembly process is also strongly dependents on solvent and concentration used.

2.3 Nanotubes of C$_8$S$_3$ according to literature

3,3'-bis(2-sulphopropyl)-5,5',6,6'-tetrachloro-1,1'-dioctylbenzimidacarbocyanine (C$_8$S$_3$ for short) is a amphiphilic cyanine dye molecule. According to literature, C$_8$S$_3$ self assembles into double-walled cylindrical nanotubes, as shown in Figure 2.4b on the next page. This molecule has some interesting properties for organic photovoltaics.[Ber+02]

2.4 Nanotubes of C$_8$S$_3$ in CG-Martini

Morphologies of J-aggregates are hard to measure and predict, because there are many variables. Computational methods could give more insights in the self-assembly process, which could help organic photovoltaics to the next level.
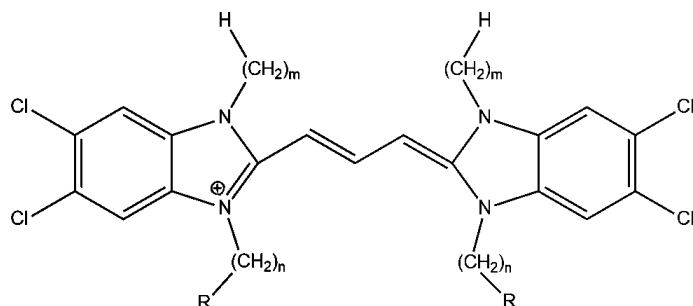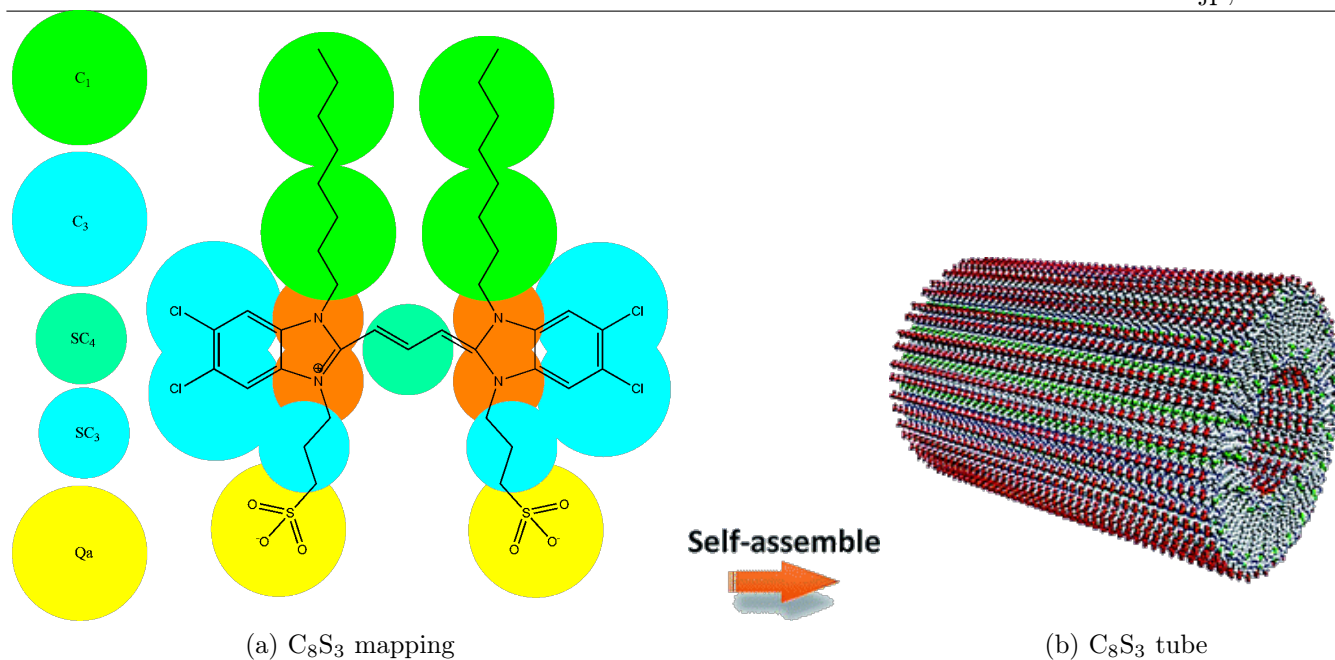
(a) C_8S_3 mapping

(b) C_8S_3 tube

Figure 2.4: Elaboration on the molecule C_8S_3.
(a) The C_8S_3 molecule. In color: CG-Martini-mapping. In black: the underlying atomic structure.
(b) The molecule self-assembles into a double-walled nanotube; the vesicle has an outer diameter of 13 ± 1 nm and inner diameter of 6 ± 1 nm. The nanotubes are micrometers long.
Source: [Ber+02]

Ilias Patmanidis of the molecular dynamics research group of the Rijksuniversiteit Groningen is working on the self-assembly process of C_8S_3. As indicated in Table 1 on the preceding page, these molecules should self-assemble into double-walled nanotubes. Until now, molecular dynamics simulations did not manage to reproduce this result. In the simulations, it forms amorphous aggregates, but double-walled nanotubes are relatively stable if built.

Coarse grained simulations reduces the computational effort per volume for MD simulations, this is interesting for bigger and longer simulations. In order to get reliable results on the stacking orientation, the model of C_8S_3 needs to be reliable. The Martini 2-model of C_8S_3, see still has some problems:

- (1) **The wrong mass of the molecule.** In Martini 2, C_8S_3 is modeled with 10 normal beads and 7 small beads. This means $10 \times 4{:}1 + 7 \times 3{:}1 = 61$ heavy atoms, instead of the 55 heavy atoms present in C_8S_3.

- (2) **The wrong stacking distance.** In Martini 2, two aromatic rings of two C_8S_3 molecules are ideally 4.5 Å apart, but according to the X-ray diffraction pattern, the aromatic rings are separated by 3.5 Å.

  Paulo Telles de Souza is developing the next version of Martini; `MARTINI 3`.

`MARTINI 3` includes a new subclass of beads: the tiny bead, as discussed in section 1.2.3 on page 7. This will solve the problems encountered in the Martini 2 model.

Coarse grained simulations will give results, but not necessarily every result is a reliable result. Before `MARTINI 3` is used to study unknown systems, it should be investigated if `MARTINI 3` can reproduce

a result with from literature with high scientific consensus, e.g. HPHC. It might be that C_8S_3 is beyond the limits of `MARTINI 3` and any other molecular dynamics force field.

2.5   Nanotubes of HPHC...

According to an article of Jonathan P. Hill in 2004, hexa-peri-hexabenzocoronene (HPHC) should self-assemble to a double-walled nanotube, as shown in Figure 2.5a, by using THF as solvent. If water was added, the tube opens, and a helix becomes visible by transmission electron microscopy (TEM), see 2.5b. The article got cited 793 times[Hil+04].
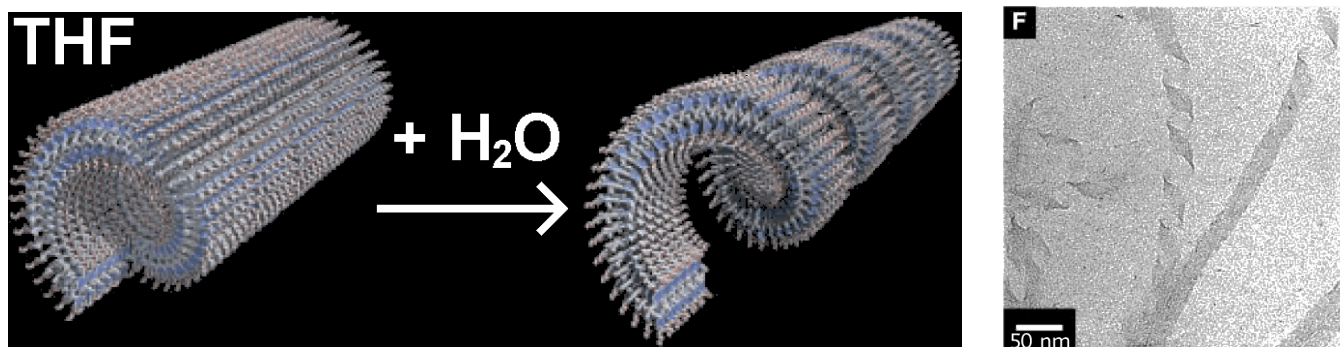
(a) HPHC self-assembles into double-walled nanotubes in THF. By adding H_2O to the solution (upto 20%), the tube opens up to reveal the morphology.

(b) The morphology is confirmed by TEM

Figure 2.5: The vesicle of the literature. (a) schematic, (b) measured. Source: [Hil+04]

The aim of this bachelor research thesis is to reproduce the result from literature with a molecular dynamics (MD) simulation, using a coarse grained model of HPHC. This is a first step to investigate whether self-assembly to double-walled nanotubes is possible with CG-Martini.

If `Martini 3` manages to model this self-assembly process with a big molecule like HPHC, smaller models can be tested, like those shown in Figure 2.6. This series will eventually end at a structure that is extremely similar to C_8S_3. If straight π-stacking fails in C_8S_3, this series will hopefully give more information about aromatic amphiphile requirements, e.g. a minimal size of the nanodisc.

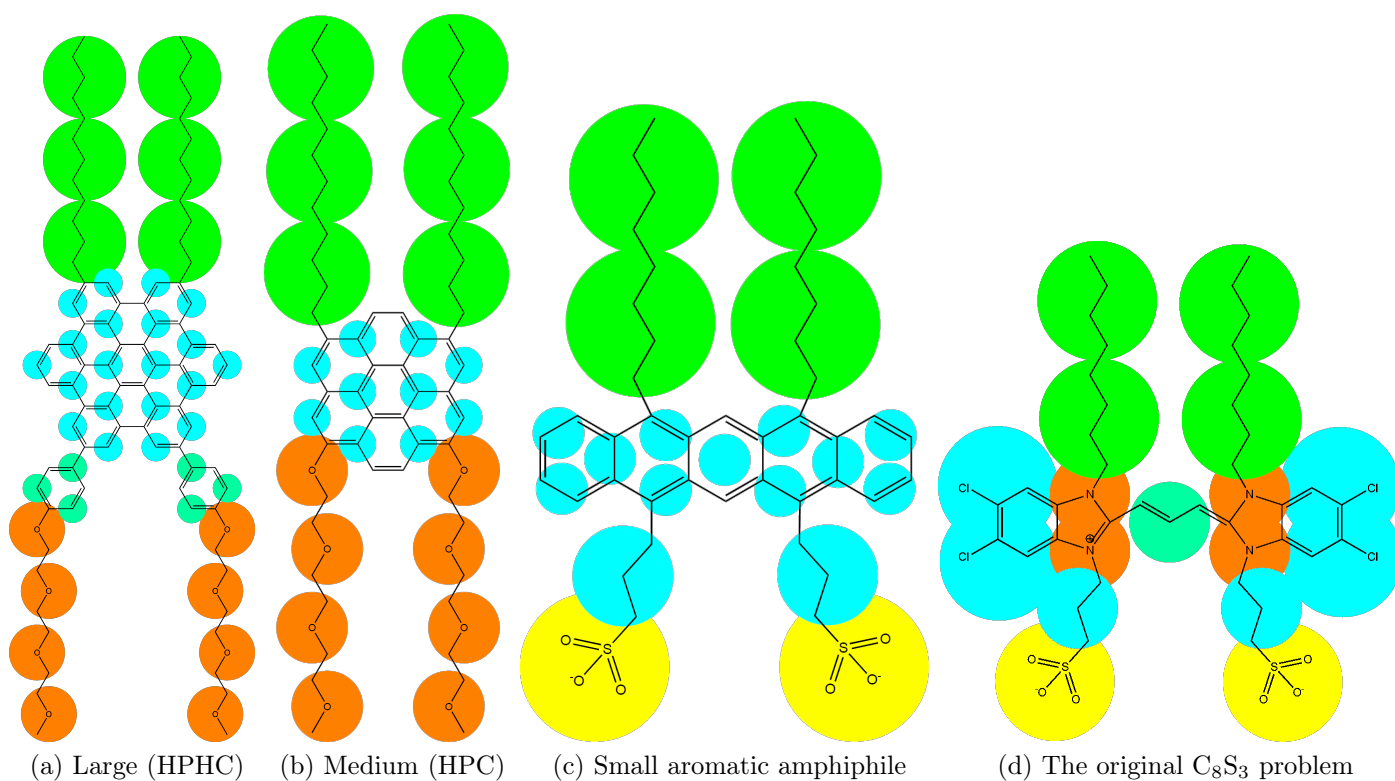(a) Large (HPHC)   (b) Medium (HPC)   (c) Small aromatic amphiphile   (d) The original C_8S_3 problem

Figure 2.6: The nanodisc amphiphile series, ranging from (a) large nanodiscs (HPHC) to (d) C_8S_3.
(a) Hexa-peri-hexabenzocoronene (HPHC).
(b) Hexa-peri-coronene (HPC)
(c) Pentacene with the same substituents as C_8S_3
(d) The problematic cianide dye (C_8S_3).

3 Methods

During this Bachelor-thesis, GROMACS 5[Abr+15] was used.

Atomistic reference parameters were obtained from the **A**utomated **T**opology **B**uilder (**ATB**)[Mal+11]. The `GROMOS 54A7` force field[HLG11] files were downloaded.

In the `md.mdp` file, the Berendsen thermostat[BSD95] was used with a temperature of 300 to 320 K. The pressure was usually 1 bar, until this gave problems with boiling THF. The pressure was then increased to 10 or 100 bar.

The trajectories were viewed with **V**isual **M**olecular **D**ynamics (**VMD**)[HDS96].

The `em.mdp` and `md.mdp` used were inspired on the `GROMACS5`-tutorial on the Martini-website:
`http://www.cgmartini.nl/index.php/tutorials-general-introduction-gmx5/bilayers-gmx5`.

`em.mdp` for AA/CG systems:
`https://www.dropbox.com/s/gueq3ch37pguuk2/em.mdp?dl=0`

`md.mdp` for AA systems:
`https://www.dropbox.com/s/w0bg5t5ph5v5hqd/md_AA.mdp?dl=0`

`md.mdp` for CG systems (note: dt = 10 fs)
`https://www.dropbox.com/s/03twpfmsojd2lob/md_dt=10fs.mdp?dl=0`

`martini_v3.0.2.itp` version used:
`https://www.dropbox.com/s/533vuc99idc2nt5/martini_v3.0.2.itp?dl=0`
Note that it is always recommended to work with the latest version of martini 3. If the simulation crashes because pairs are undefined, define pairs by copy-pasting everything below [`nonbond_params`] to a new definition: [`pairtypes`]. This should make it work.

3.1 Suggestions for Improvements

If the research is continued, the following things could be improved.

Pressure-coupling.

In the `md.mdp`-file used for CG simulations, the pressure-coupling was set to parrinello-rahman, and the thermo-coulping to Berendsen. Sometimes, equilibration turned out to be troublesome, especially for constraints and membranes.

In Appendix D.1 on page 42, the combination of Berendsen pressure- and thermo-coupling is tested. These settings appear more stable, and are therefore recommended for future simulations.

4   Experiments; Results and discussion

First, the model is validated. Then, self assembly to nanowires and nanowire aggregates is simulated. Finally, a HPHC membrane is simulated and attempts to bend the membrane are done. This will give an indication on the feasibility of double-walled nanotubes to form.

4.1   Modeling & validation

4.1.1   Modeling

Step 1: Several coarse grained (CG) models of Hexa-peri-hexabenzocoronene (HPHC) were proposed. The selected CG model of HPHC has the same symmetry (C_{2v}) as HPHC, see Figure 4.1.

Step 2: Interesting fragments of the molecule were selected and submitted to the Automated Topology Builder (ATB). These all atom (AA) models were used as building blocks for the validation process, see Section 4.1.2. The bonded parameters of the CG models were optimized, i.e. the distributions of the CG model resemble the AA model as close as possible. For the fragments, see Figure 4.2. The optimization process will be discussed in 4.1.2 on the next page.

For some molecules, multiple mapping styles, are possible. In section 4.1.3 on page 19, two different CG models of coronene are used, but with different purposes.

$C_{92}H_{102}O_8$

100 heavy atoms
40 beads
6x 4:1 = 24 atoms
8x 3:1 = 24 atoms
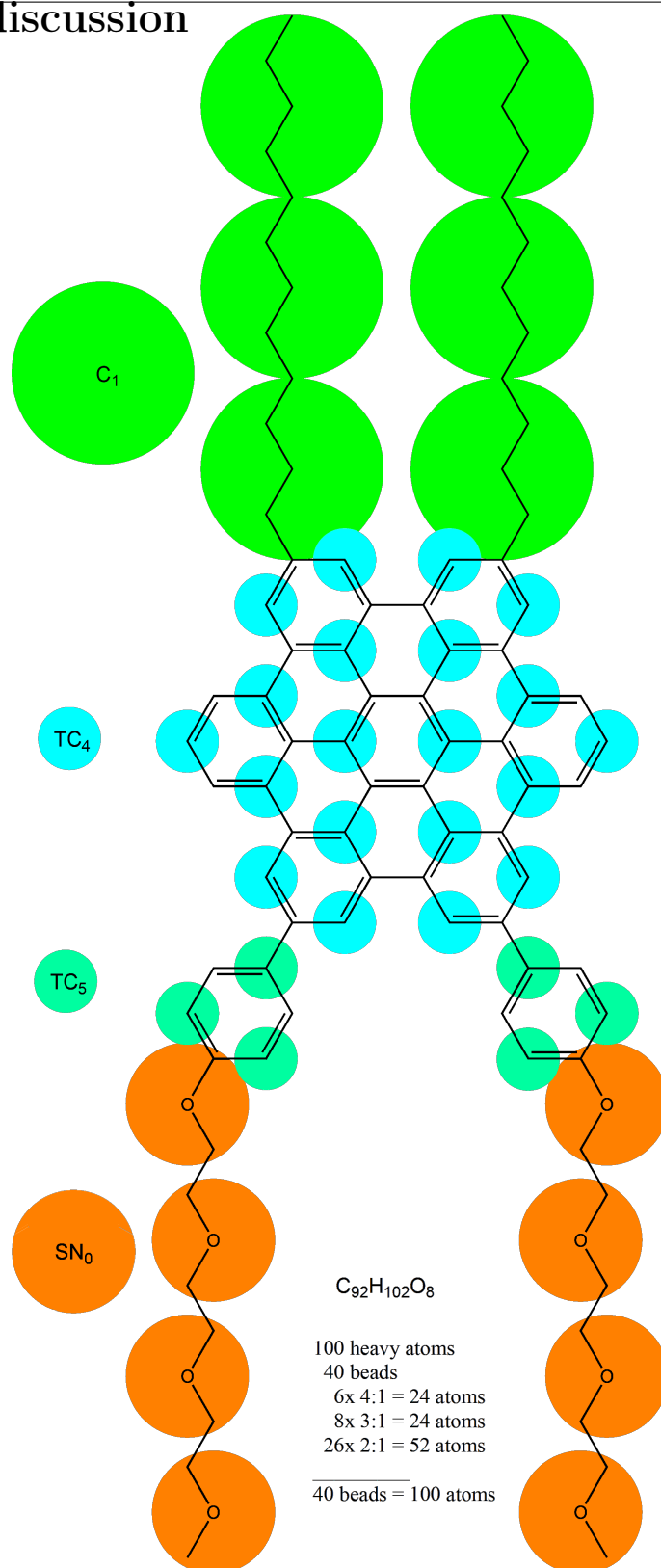26x 2:1 = 52 atoms
_____
40 beads = 100 atoms

Figure   4.1:   Hexa-peri-hexabenzocoronene (HPHC). In colors: CG mapping, in black: the underlying atomic structure.
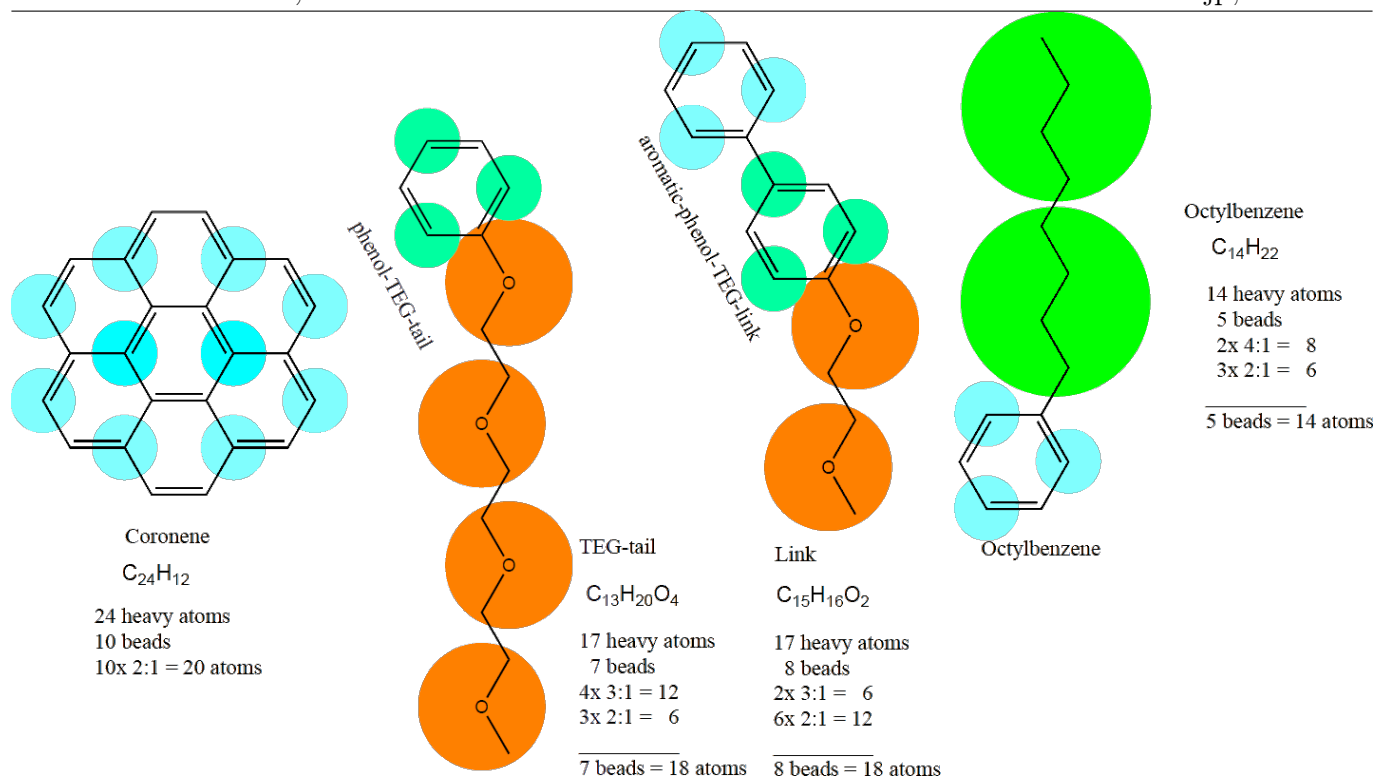
Figure 4.2: Fragments that were used to optimize and validate bonded parameters for the HPHC molecule.

4.1.2 Validation & Optimization

A tutorial from the Martini-website[3] was used
as experimental procedure. The tutorial was written for `GROMACS 4`, but for this bachelor research project, `GROMACS 5 (2016)` was used, so commands like `g_angle` changed to `gmx gangle` and so on.

Atomistic models were build and submitted to the ATB-server to obtain All Atom (AA) GRO-MOS54A7 force field parameters, as described in section 4.1.1. These All-Atom (AA) models were put in a box of 5 by 5 by 5 nanometer[4], energy minimized[5], dissolved in THF[6], energy minimized, and simulated for 5 ns (dt = 2 fs ; nsteps = 2.5 milion).

Because there are many fragments to be analyzed, most of the work was automated via bash-scripts. Initially, scripts were mainly for doing the analysis and making indexfiles, but eventually nearly everything was automated[7].

The AA-trajectory was converted to a coarse-grained trajectory by using the `convert`

The "`traj_AA_mapped_as_CG.gro`" file was analyzed with the `calcdists.sh` script. The distributions were overlayed distributions for the equivalent bonds, angles and dihedrals of the with CG models.

---

[3]`http://www.cgmartini.nl/index.php/tutorials-general-introduction/martini-tutorials-polymers`, visited in April 2017

[4]gmx insert-molecules -f single_molecule.gro -box 5 5 5 -nmol 20 -o 20dry.gro

[5]gmx grompp -f em.mdp -c 20dry.gro | mdrun -v -c 20dry.gro

[6]gmx solvate -cp 20dry.gro -cs THF_AA.gro -o 20THF.gro

[7]Most scripts can be found in the appendix; for analysis scripts: see A.1 on page 36

The `CG.itp`-files were made in google-sheets, an online version of excel. This spread-sheet allowed to keep track of used parameters. Together with the collection of graphs, the spreadsheet helped to make rational decisions on how to improve the model. The validated pieces were easily put in place in the final model.

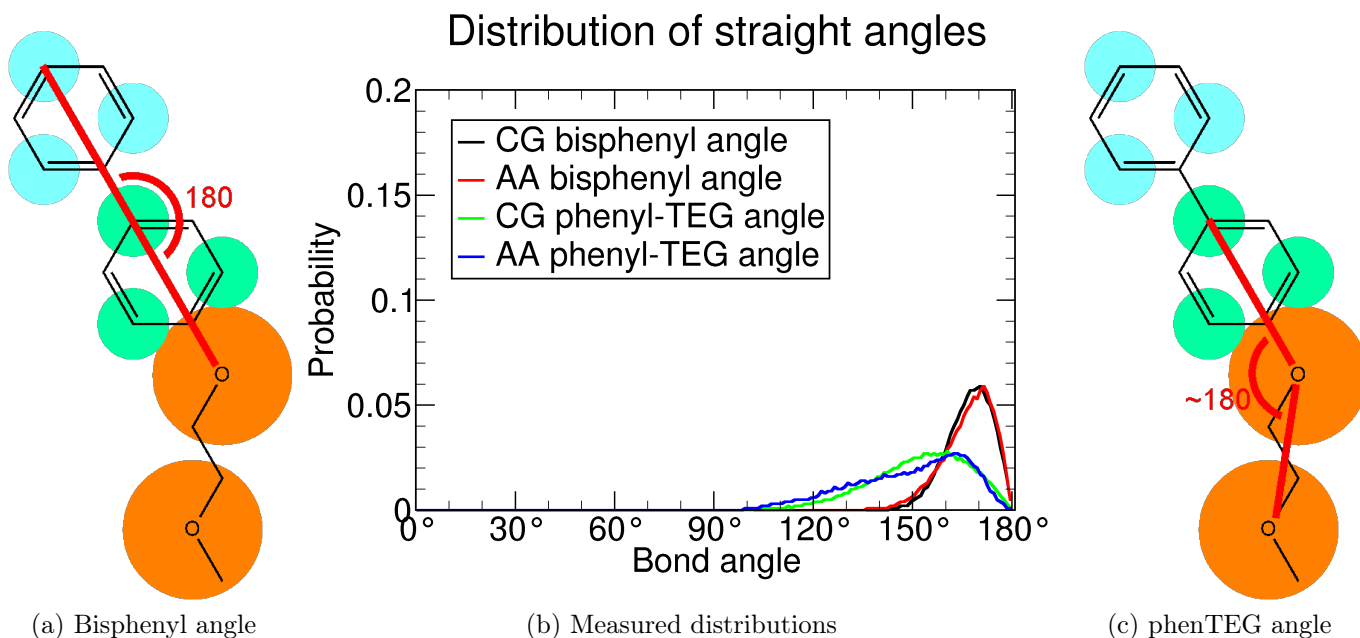(a) Bisphenyl angle   (b) Measured distributions   (c) phenTEG angle

Figure 4.3: The bisphenyl and phenTEG angles were accepted.

Each fraction was used to optimize different bonded parameters. There were 13 bond types, 11 angle types, and 5 dihedral types.

More distributions are shown in the appendix, see C on page 39. The bisphenyl dihedral of the molecule shown in Figure 4.3, is elaborated in Appendix C.2 on page 41.

According to the distributions, all aromatic bonds should be modeled with constraints. A model in which all bonds in the aromatic nanodisc are replaced with constraints is, however, a useless model. A simulation becomes unstable if a constraint is unsatisfied. If all bonds of Figure 4.5b on the next page were constraints, the simulation crashed due to "links errors", so bonds were used instead of constraints.

Hexabenzocoronene (HBC) modeling

Note that in Figure 4.1 on page 15, the beads of hexabenzocoronene are drawn on the carbon atoms. This would mean that the bond length between two beads in the center of hexabenzocoronene model (**blue lines** in Figure 4.4a) would be longer than the rest of the bonds in the aromatic nanodisc (**black lines** in Figure 4.4a) as drawn in Figure 4.4a. This would mean that there is a region of low bead density in the center of the coarse grained hexabenzocoronene model.

In order to create a homogeneous distribution of the beads in the HBC nanodisc, all nanodisc-bonds were set to be equal in length. Note that the bondlength was increased from 0.24 nm of the all atom simulation to 0.267 nm, which is closer to the benzene-bondlength of 0.285 nm, and still gave a reasonable disc diameter (diameter is 1.19 nm for the CG model vs 1.125 nm for the AA model.).

(a) The first sketch in which the center of mass of the beads are on carbon atom positions.
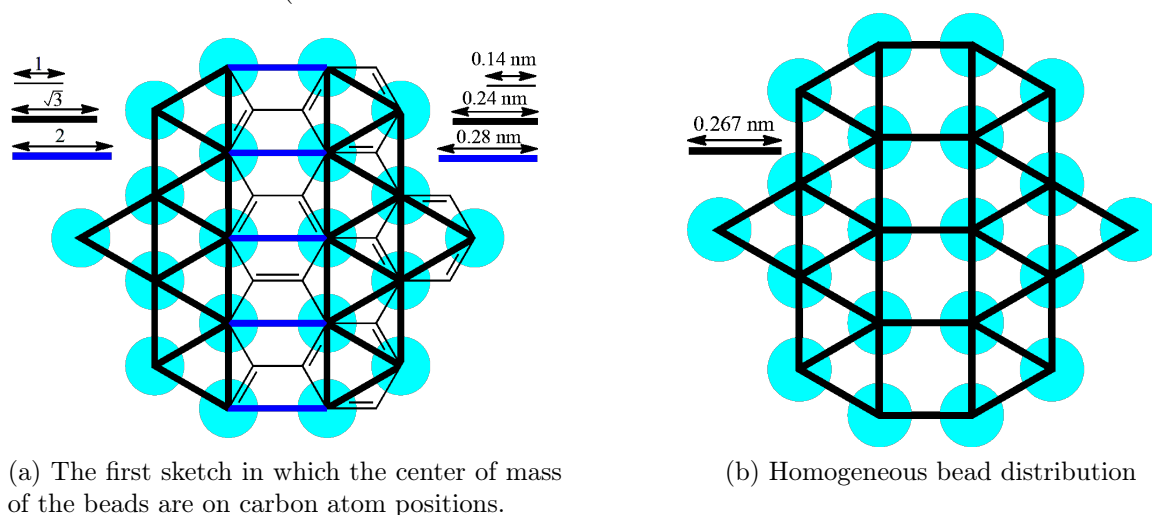
(b) Homogeneous bead distribution

Figure 4.4: Mapping of hexabenzocoronene: the beads are not exactly on the carbon atom positions, because this would cause a gap of low bead density in the center of the nanodisc.

The hexabenzocoronene (HBC) nanodisc is defined without dihedrals, because there are too many ways to define them. There are many alternatives, e.g. by defining angles that should be 120°, or by defining long bonds, e.g. as shown in Figure 4.5c. There are multiple combinations of parameters that provide the same stiffness to the coarse-grained model, as the all-atom-HBC model, and run stable with a timestep of 20 fs. Unfortunately there was too little time to develop it completely; not all stable settings in HBC are stable in HPHC too. The HPHC model used was stable with a time-step of 10 fs.

Appendix C.1 on page 39 shows the validation of the stiffness of HBC. Appendix D.2 on page 43 contains the latest discoveries on HBC modeling.

(a) Angle network

(b) Bonded network

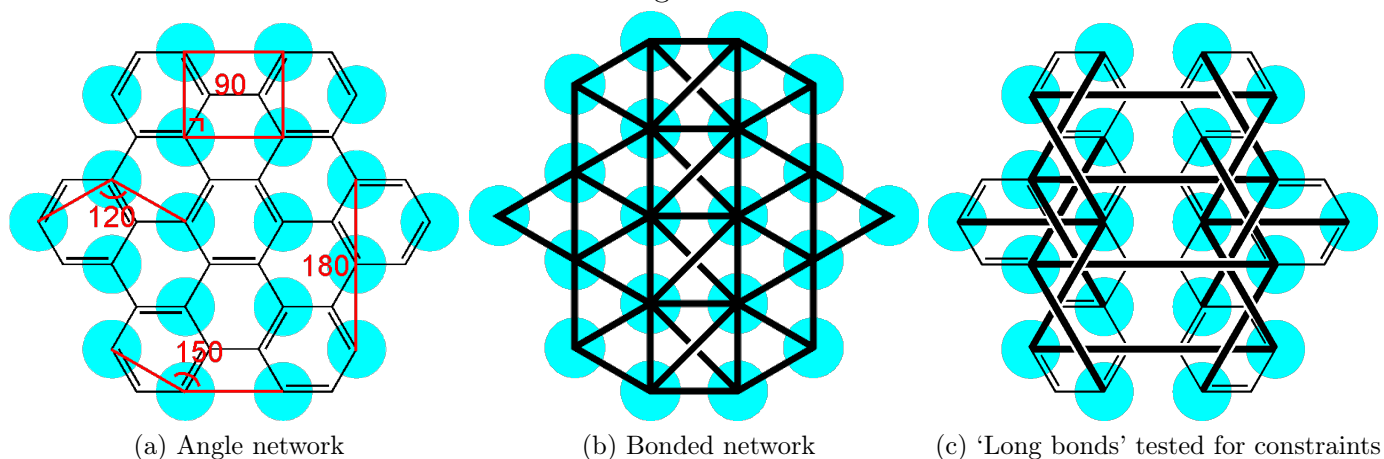(c) 'Long bonds' tested for constraints

Figure 4.5: Various definitions of bonds and angles in hexabenzocoronene. Together, this combination of parameters ensure that hexabenzocoronene is flat and stable.

4.1.3   The fundamental $\pi-$stack in coronene

When inspecting the trajectory of the all atom simulation, it was noticed that the molecules associate and dissociate from each other reversibly.

The main driving force behind the aggregation is the $\pi - \pi$ stack of the super aromatic center. Hexabenzocoronene has d_{6h}-symmetry, just like coronene and benzene. When coarse graining with tiny beads (TC3; 2:1 mapping), the coarse grained models of these super aromatic compounds have d_{3h}-symmetry.

The driving force of aggregation of coronene was tested, using model B of Figure 4.6.

20 molecules of coronene were simulated in a box of 5 by 5 by 5 nm, in 3 different situations:

- (1) AA coronene with AA THF,

- (2) CG coronene in Martini 3 THF,

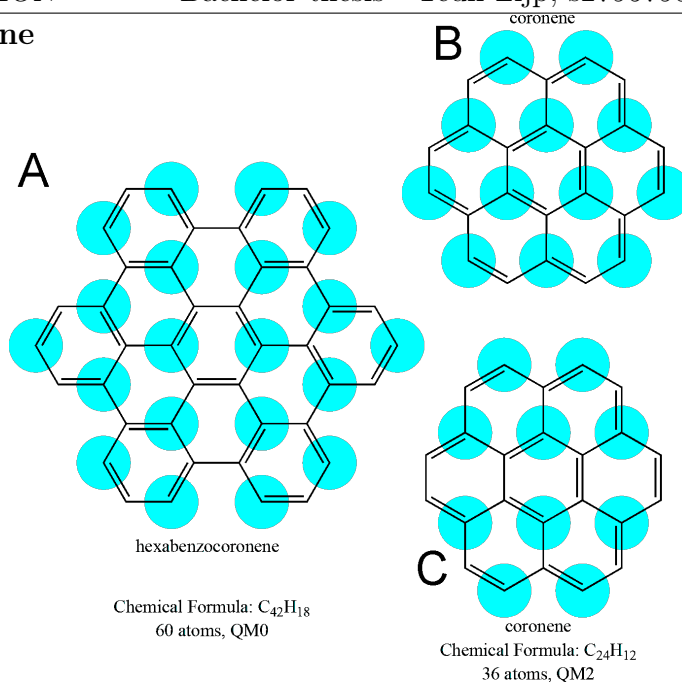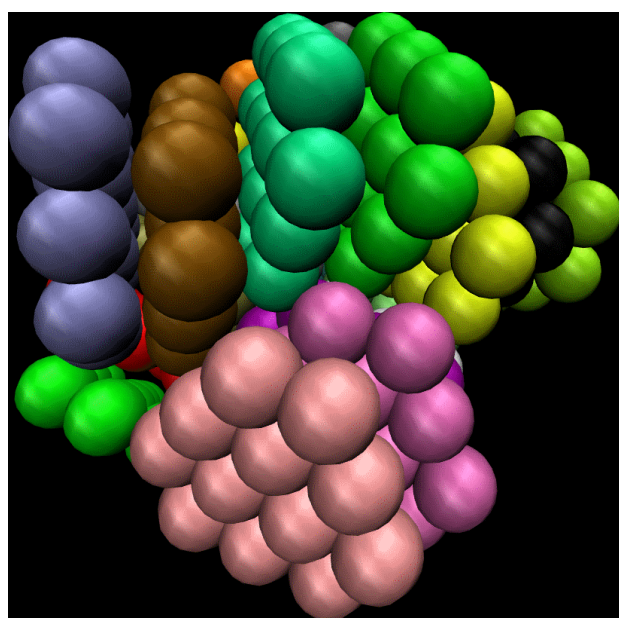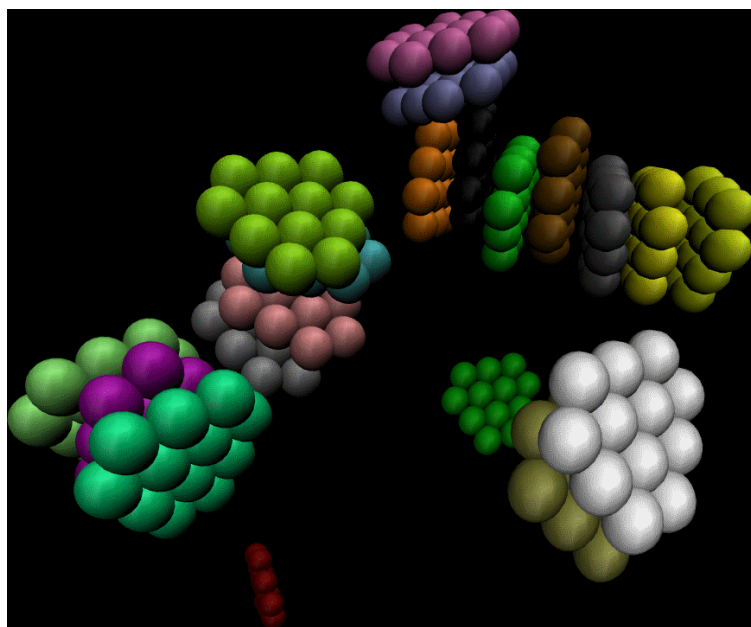- (3) CG coronene in Martini 3 water (WN).

Figure 4.6: Modeling the aromatic parts. (A) Hexabenzocoronene. (B) Coronene, used for testing the solubility and aggregation. (C) Coronene, used for testing the bonded parameters in hexabenzocoronene.

(a) Coronene in water   (b) Coronene in THF

Figure 4.7: Coronene in different solvents. (a) in THF, Coronene forms strands that constantly associate and dissociate. (b) in water, Coronene forms ball-shaped clusters.

In water, coronene does not dissolve. After approximately 0.1 ns all 20 coronene molecules are aggregated, and start to form a ball, see Figure 4.7b. The ball is a stable structure: it does not dissociate. Inside the ball, molecules are lightly packed into a few stacks. Inside the ball, molecules

shuffle around: molecules change neighbours every now and then. This would mean that the coronene ball of Figure 4.7a is actually a liquid droplet.

Alex de Vries wrote a script to analyze the stacks formed: `MAKECLUSTEREDTRAJ.sh`. The output of this script is a `clusterData.dat` file, in which the number of clusters and the size of each cluster are listed. The most trivial first step is to plot the number of clusters as a function of time, see Figure 4.8a on the following page: if the same number of molecules is distributed over fewer stacks, the average size of the stacks is bigger. This should give a first estimate on the extend of aggregation. This method is elaborated below in Paragraph 4.1.3.2. There are better tools than the first estimate; see all methods elaborated below.

4.1.3.1   Example Data Set.   clustSize = (17, 1, 1, 1)

If there is one long stack of 17 molecules and three loose molecules, the system is nearly completely aggregated. Various statistical tools will be used to analyze test this data set, this allows us to compare different statistical tools with each other. In the end, a rational decision can be made when to use what tool.

4.1.3.2   (Arithmetic) Average cluster size.

The average cluster size is the sum of the clustSizes, divided by the number of clusters, see Eq. 4.1.

Note that the sum of the clustSizes adds up to the total number of molecules present in the system.

$$\text{Average clust size} = \frac{1}{\text{nr. of clusters}} \sum_{i=1}^{\text{nr. of clusters}} (\text{clustSize})_i = \frac{\text{nr. of molecules}}{\text{nr. of clusters}} \qquad \text{(Eq. 4.1)}$$

In the example data set mentioned above, there are 4 clusters that together contain 20 molecules, so the "average clust-size" is $\frac{20 \text{ molecules}}{4 \text{ clusters}} = 5$ molecules per cluster, which does not sound like a nearly fully aggregated state. The fact that the "average clust-size" gives a poor estimate of the extend of aggregation can be explained with the fact that it does not keep the size of the individual clusters into account.

The only reason to use the average clust-size is because it is extremely easy to obtain all required data for this. The number of molecules is fixed when starting the simulation, and the number of clusters can be obtained with a gromacs-tool: `gmx clustsize`[8], which is readily available. Alternatively, it can be computed with `MAKECLUSTEREDTRAJ.sh` script. Either way the output is plotted in Figure 4.8a on the following page.

4.1.3.3   Weighted average cluster size.

The weighted average is calculated by multiplying each occurring $(\text{clustSize})_i$ with a weight.

For clusters, it makes sense to put a bigger weight on bigger clusters. In Eq. 4.2, each occurring clustSize)$_i$ is given its own value as a weight, resulting in $\sum_{i=1}^{n} (\text{value})_i \times (\text{weight})_i = \sum_{i=1}^{n} ((\text{clustSize})_i)^2$, see Eq. 4.2 in the numerator.

Note that the weights should be normalized: the sum of the weights should be equal to 1. In Eq. 4.2, normalization is done afterwards: the "unnormalized weighted average" is divided by the sum of the weights, i.e. weighted average $= \frac{\sum_{i=1}^{n} (\text{value})_i \times (\text{weight})_i}{\sum_{i=1}^{n} (\text{weight})_i}$. The sum of the weights becomes the sum

---

[8]`http://manual.gromacs.org/programs/gmx-clustsize.html`

of the clustSizes, which is the total number of molecules present in the system, see Eq. 4.2 in the denominator.

$$\text{Weighted average clust size} = \frac{\sum_{i=1}^{n}((\text{clustSize})_i)^2}{\sum_{i=1}^{n}(\text{clustSize})_i} = \frac{\sum_{i=1}^{n}((\text{clustSize})_i)^2}{\text{nr. of molecules}} \qquad \text{(Eq. 4.2)}$$

in which n is the total number of clusters.

The "weighted average clust-size" of the example data set is $\frac{17^2+1^2+1^2+1^2=292 \text{ (molecules}^2)}{20 \text{ molecules}} = 14.6$ molecules per cluster. The weighted average gives a better measure of the extend of aggregation, because it keeps the size of each cluster into account.

The weighted average cluster size was computed as a function of time, by using the output of MAKECLUSTEREDTRAJ.sh (clusterData.dat lists the size of each cluster), see Figure 4.8b.

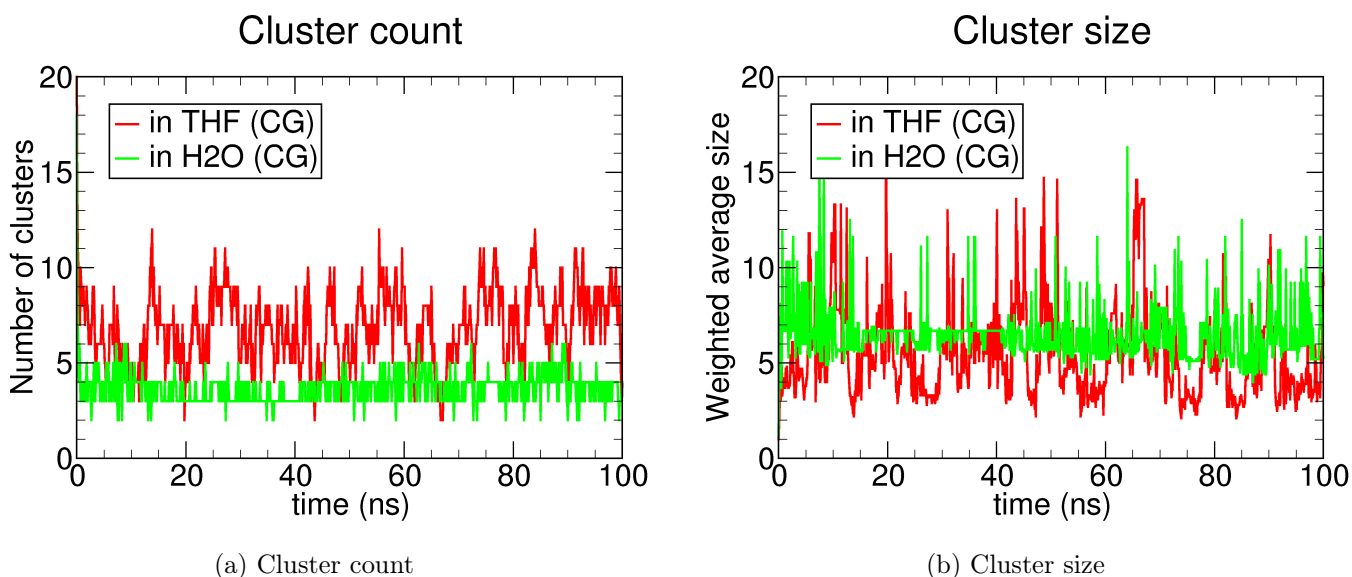
(a) Cluster count

(b) Cluster size

Figure 4.8: Cluster analysis as a function of time.
In (a) the number of clusters are counted in each frame of the simulation. The inverse of this plot is proportional to the average cluster size. From this graph, the extend of aggregation appears greater in water than in THF, because are more coronene clusters in THF than in water, i.e. the size of the clusters are greater in H_2O.
In (b) the weighted average cluster size is calculated in each frame of the simulation. From this graph, aggregation seems more dynamic in THF than in water, but it is hard to draw a conclusion on the extend of aggregation.

Though the weighted average is a theoretically good measure, the plot obtained in Figure 4.8b still doesn't provide clear information on the extend of aggregation. The biggest flaw made is that the analysis is done on a frame-by-frame basis. It may be better to combine the data into one (or a few) data-set(s), and make histograms.

4.1.3.4   Histograms.   Histograms were made for cluster size in the two different solvents; the data was split in 4 sets to check how the distribution evolves over time, see Figures 4.9b and 4.9a. Fortunately, the difference is little; the distributions overlap, so it is allowed to pool the 4 sets, see Figure 4.9c.

(a) Coronene in water   (b) Coronene in THF   (c) Pooled distributions
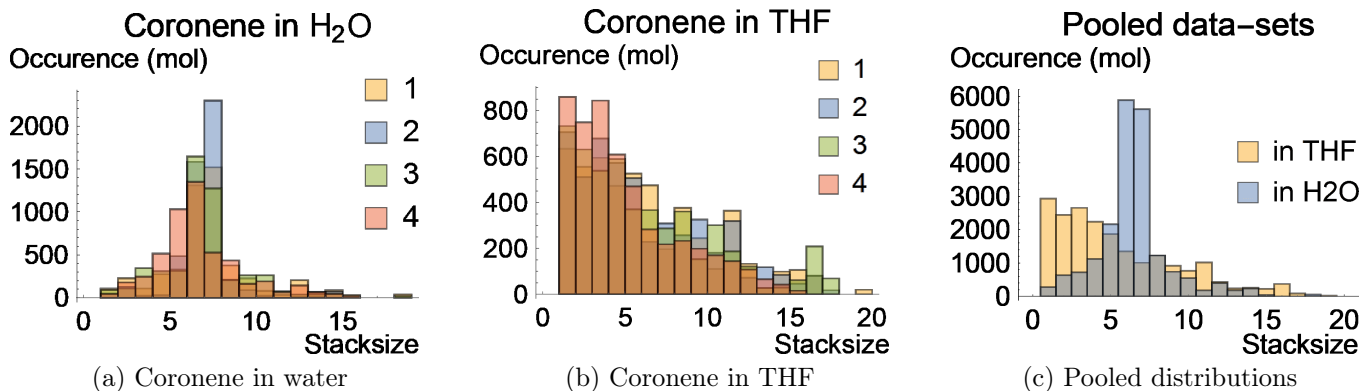
Figure 4.9: Cluster histograms. Cluster analysis gives one large data-set detailed information about the clusters found in solution. (a) and (b), are used to check whether the distributions evolve over time. Because the distributions overlap significantly, the sets can be pooled to one data set, see (c). (c) A histogram of the individual cluster sizes of all frames of the simulations. This histogram should give more information on the extend of aggregation, but it also gives away a hint: for some reason, there mainly stacks of 6 or 7 coronene molecules in H_2O.

The histogram of coronene cluster-size in the two different solvents (H_2O vs THF) are completely different. This mainly has to deal with the fact that there are two different phenomena at play in the different solvents.

When two aromatic molecules meet, interact via the π-cloud, and travel together, the Gibbs free energy of that process is $\Delta G_{\text{aggregation}} = \Delta H - T\Delta S$. The π-π-interaction is generally enthalpically favourable ($\Delta H_{\text{aggregation}} < 0$). Note that there is an entropic penalty ($-T\Delta S_{\text{aggregation}} > 0$), because two molecules move together as one; thermal energy needs to be distributed over fewer translational states. Therefore, there are cases in which aggregation is unfavourable ($\Delta G_{\text{aggregation}} > 0$).

According to literature, coronene does not dissolve in water; ($\Delta G_{\text{aggregation}} << 0$).
    When 20 coronene molecules are in water, the coronene molecules try to avoid contact with H_2O as much as possible. The most efficient way to do so is when the surface is a sphere. This is exactly what was observed in Figure 4.7a on page 19. The cluster-size distribution in H_2O shown in Figure 4.9c tries to tell us that the ball of Figure 4.7a is mainly 6 or 7 coronene-molecules across.

According to literature, coronene is soluble in THF; ($\Delta G_{\text{aggregation}} > 0$).
    The distribution of coronene-clusters in THF is roughly similar in shape to a Boltzmann distribution for a slightly endothermic process, e.g. rotational energy states. Probably $\pi - \pi$-stacking is unfavourable because the enthalpy is less than the entropic penalty, i.e. $\Delta G_{\text{aggregation}} = \Delta H - T\Delta S > 0$. Note that the processes is only slightly unfavourable, so the aggregation process is not forbidden. If the solution is diluted, the probability of finding aggregates will decrease, i.e. coronene will dissolve.

4.1.4   Collection of Validated Parameters

The validated parameters for the HPHC model can be found and downloaded in Appendix B on page 37.

4.2 Self-assembly of coarse grained HPHC

Now that the model of hexa-peri-hexabenzocoronene (HPHC) is validated, MD simulations can be started. The hypothesis is that HPHC self-assembles into a supramolecular structure: double-walled nanotube.

    The first step is to simulate HPHC at various concentrations, to observe aggregation of HPHC to nanowires. Step 2 is to simulate two nanowires in a box to form nanowire aggregates, in which the wires interact via the aliphatic tails to form a dimer. The third step is to make a membrane, and in the last step, the membrane is bend to a double-walled nanotube.

4.2.1 Self-assembly step 1: Nanodisc π -stacking

When 20 HPHC molecules were simulated in a box of $5 \times 5 \times 5$ nm for 0.2 μs, the simulations costed little computational effort, so that the simulation was finished the same working day. The HPHC molecules started self-assembly to a nanowire, until the point at which the nanowire started to interact with the periodic image of itself, because the box was too small for a nanowire of 20 molecules long. The other HPHC molecules also started to form short nanowires, which interacted with the longer nanowire via the aliphatic tails; this starts to look like bilayer-like system, see 4.10a. This is a good result, but not good enough to build a nanotube with.
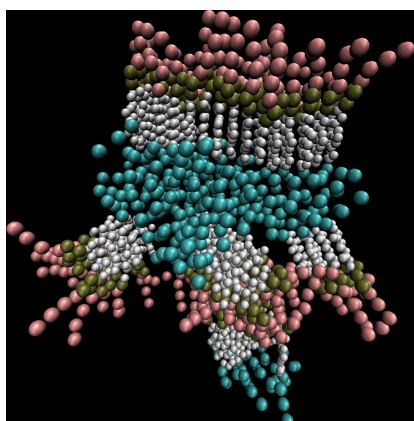
(a) Bilayer-like structures after 0.5 μs
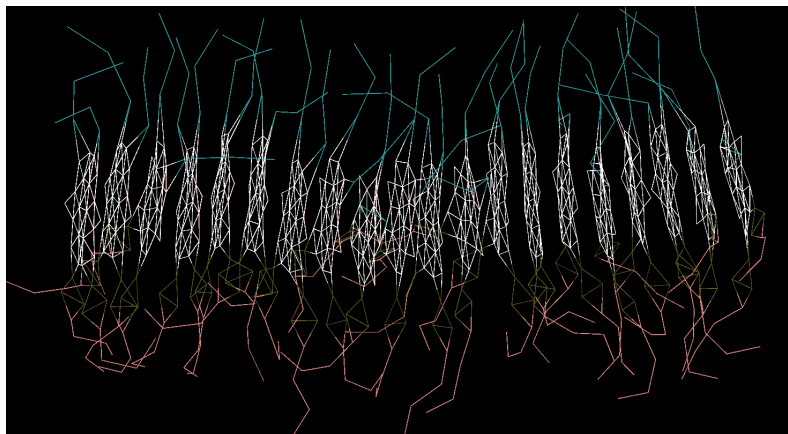
(b) Nanowire after 1.0 μs

Figure 4.10: Results of the π -stack experiment. (a) a box of $5 \times 5 \times 5$ nm with 20 HPHC molecules forms bilayer-like aggregates. Shot was taken at 0.5 μs. (b) In a box of $8 \times 8 \times 8$ nm, a nanowire is formed after 1 μs.

When 20 HPHC molecules were simulated in a box of $8 \times 8 \times 8$ nm, the simulation consumed more computational effort. The extend of aggregation was plotted as a function of time, see Figure 4.11 on the following page. After 1 μs, a stack of 20 HPHC molecules formed, see Figure 4.10b. This structure was saved as `1clust.gro` and was used in the next step. The unit cell dimensions of `1clust.gro` was inspected, and it turned out that one stack of 20 molecules is 7.45 nm high, meaning that the average distance between 2 nanodiscs is approximately 0.37 nm. This is consistent with literature[9].

---

[9]π-π-stack-distance in graphite = 3.35 Å, source: `http://www.me.umn.edu/~dtraian/TonySlides.pdf` slide 4.
π-π-stack-distance in benzene = 3.6-3.8 Å, source: `http://www.scs.illinois.edu/denmark/wp-content/uploads/gp/2011/gm-2011-1_18.pdf` slide 6.

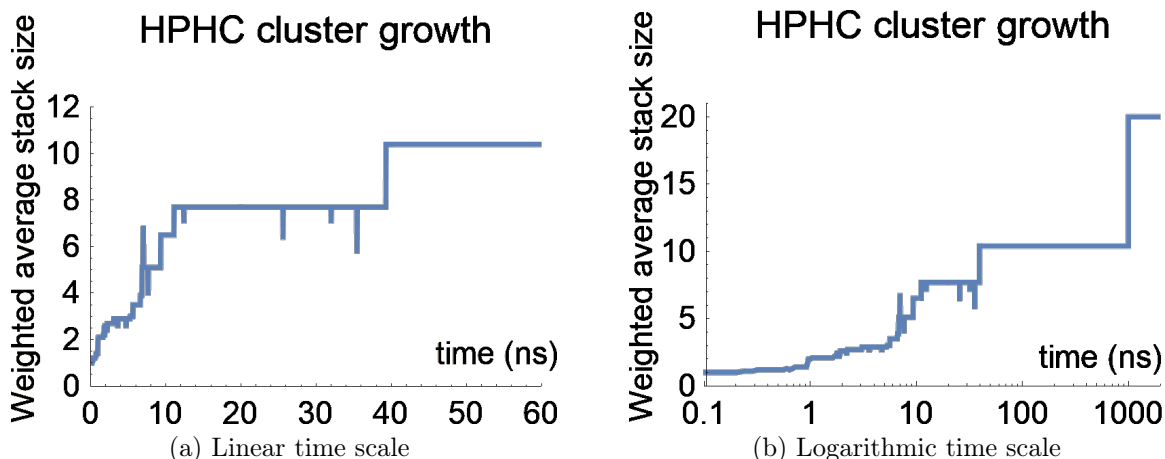(a) Linear time scale   (b) Logarithmic time scale

Figure 4.11: Cluster-analysis of the HPHC self assembly: the stacks are growing over time, until 40 ns, when two stacks are formed. It takes up to 1 μs until finally the two stacks find each other. After 1 μs there is only one stack of 20 HPHC molecules.

4.2.2 Self-assembly step 2: aliphatic tail dimers

Two stacks of 20 HPHC molecules were put in a box of $8 \times 8 \times 8$ nm. The goal was to see whether the aliphatic tails would find each other, to form a structure that looks like the cross section of a bilayer membrane. After a simulation of 1.5 μs, an infinite bilayer had formed, see Figure 4.12 on the next page. This happened because the stacks are approximately 8 nm high, so they are able to interact with periodic images of itself or the other. There was a high chance that two aromatic stack-ends would find each other to form a new π-stack. If the aromatic ends find each other, their interaction is irreversible. In Figure 4.12, both aromatic ends of the stacks interact with the aromatic end of the other stack, forming a continues stack over the periodic images; i.e. in Figure 4.12b we see one stack. this wasn't completely according to plan.

In order to prevent this infinite stacking, the box size was increased to $12 \times 12 \times 12$ nm. This increased the number of particles to be simulated by a factor of $\left(1\frac{1}{2}\right)^3 = 3.4$, which increased simulation times on the single machine. A short simulation of 0.1 μs was tried but yielded an inverted bilayer as shown in Figure 4.13a. A long simulation of 1.5 μs was done using PEREGRINE[10], it showed that the inverted bilayer was meta-stable, it converted to the normal bilayer as shown in Figure 4.13b in 0.26 μs.

---

[10]http://www.rug.nl/society-business/centre-for-information-technology/research/services/hpc/facilities/peregrine-hpc-cluster
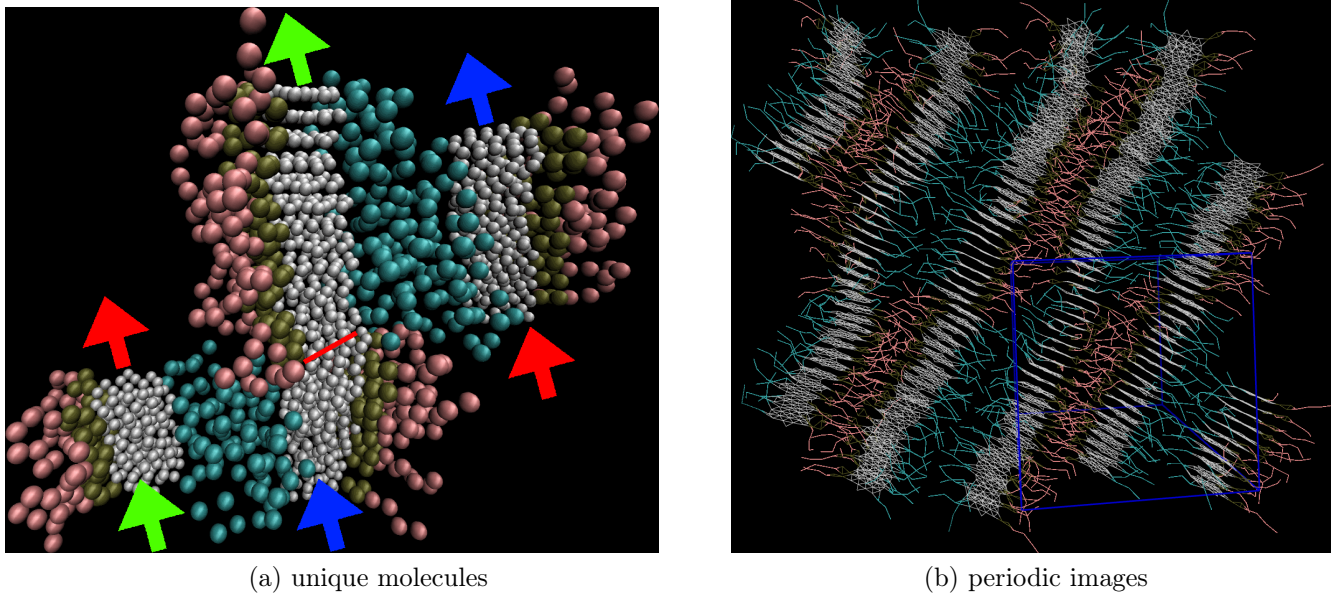
(a) unique molecules

(b) periodic images

Figure 4.12: First attempt to form a bilayer: 2 stacks of 20 HPHC molecules. The box-size simulation was $8 \times 8 \times 8$ nm.

In (a), the unique molecules are shown; the arrows indicate where the stacks continue over the periodic image. Note that green and blue connect the original stacks of 20 HPHC molecules over the periodic boundary condition; red indicates where the two original stacks have connected, this coinsides with a change in tail orientation.

In (b) the blue square in the bottom-right corner is the simulated unit cell, which is repeated as a periodic image.

(a) 20 ns → inverted bilayer
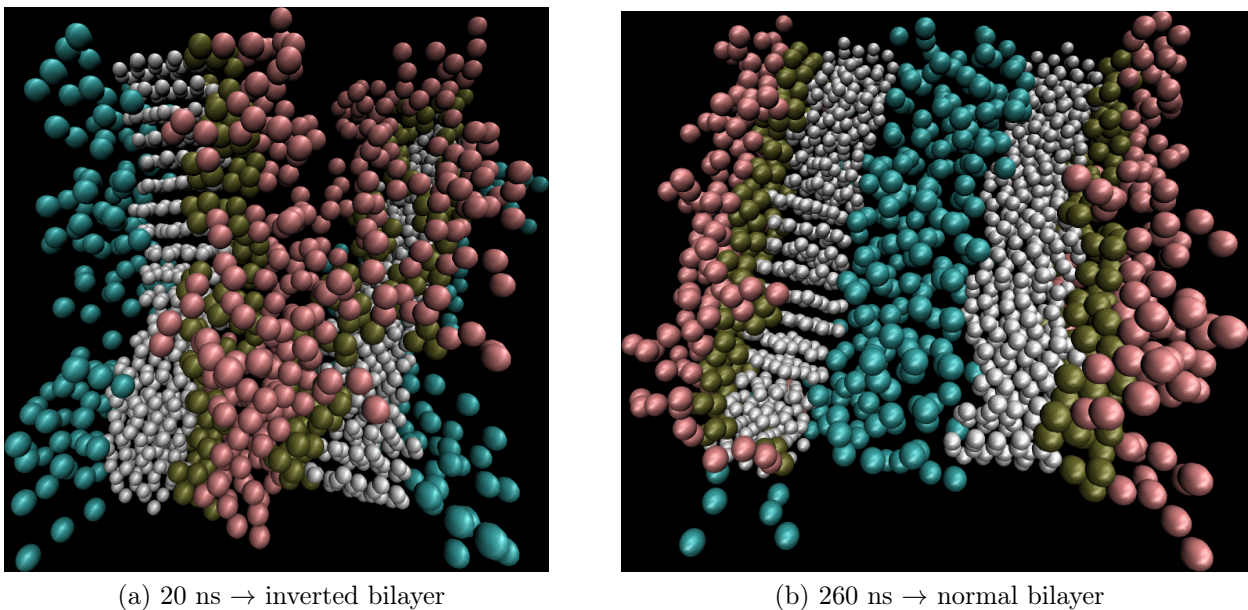

(b) 260 ns → normal bilayer

Figure 4.13: HPHC simulations that started with 2 stacks of HPHC molecules. The box-size was $12 \times 12 \times 12$ nm. Note that the inverted bilayer (a) is metastable, it is formed after 20 ns but it falls apart after 260 ns. The bilayer-like-dimer (b) appears stable, it is also observed after 1.5 μs.

4.2.3 Self-assembly step 3: Membranes

Now that the aggregation and bilayer formation are validated, the bilayer can be bent to see if a nanotube will be formed.

4.2.3.1 Using aggregated stacks as a template.
The initial idea was to put multiple copies of 4.13b on the preceding page[11] in one box to form a membane[12]. The concept was good and gave interesting results, like the tetramer shown in 4.14. Unfortunately, the tails of the dimer of Figure 4.13b are not closely packed, but spread out wide. As a result, the unitcell of the dimer could never be cut tight; there was always a lot of empty space. As a result, the HPHC dimers were always far away from each other in the starting conformation, meaning that clusters have to travel a lot before they can interact sideways. The tetramer was the only reasonable decent observed structure, the rest of the attempts
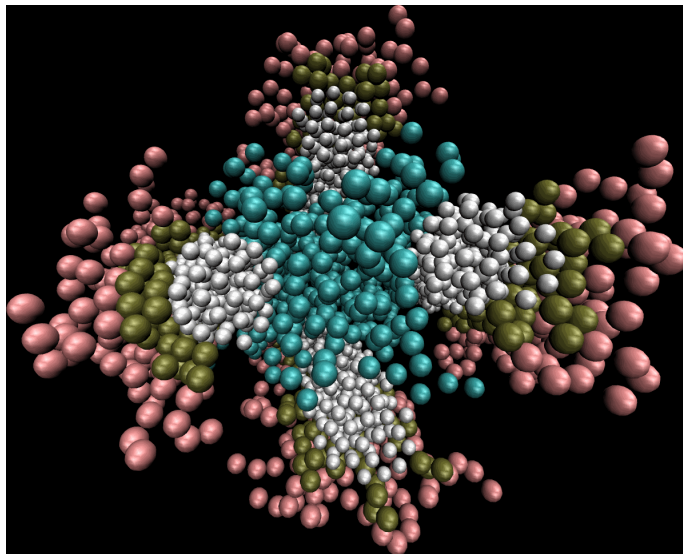

Figure 4.14: When the bilayer-like dimer of Figure 4.13b simulated in a box with a copy, this tetramer was formed.

all had a mismatch, meaning that this is not the way to build a decent membrane.

4.2.3.2 INSANE.
Tsjerk Wassenaar wrote INSANE[Was+15], a python-script that inserts proteins into phospholipid membranes (INto membrANE). For this project, Tsjerk created a test-version of INSANE that includes HPHC as a possible lipid, so that is able to produce a membrane out of HPHC molecules. Unfortunately, INSANE prefers to treat the lipid molecules as rods, which is fine for phospholipids, but definitely not for nanodisc aggregates. The main problem was that output file contains nanodiscs that are rod-like. The rods unfold during energy minimization, but their orientation is chaotic. After a few MD-simulations, the nanodiscs slowly started to form some π-stacks, and the clusters grew slowly over time, but after a few μs's the nanowires still didn't form completely, see Figure 4.15b.

Apart from the fact that the membrane formed by INSANE was disordered in the π-stack, it was also far from realistic. The aliphatic tail interaction was there, but the π-stacks of the nanodiscs is the first interaction that is formed during the self-assembly process.
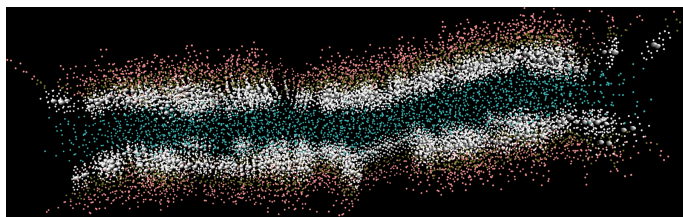
(a) Side view: correct aliphatic interactions.
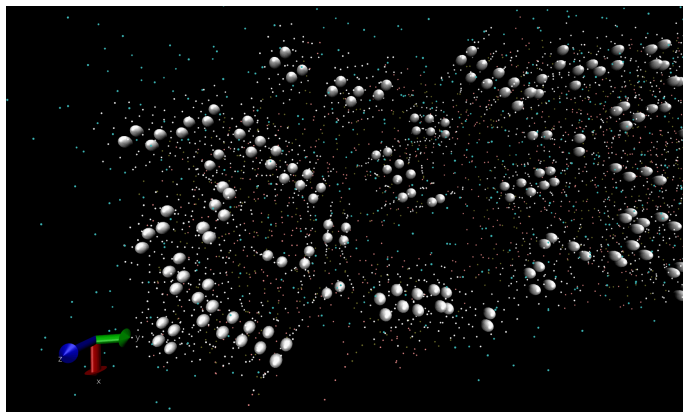
(b) Top view: broken π-stacks

Figure 4.15: The HPHC membrane created with INSANE.
(a) The INSANE membrane has correct aliphatic interactions.
(b) The INSANE membrane has broken π-stacks.

---

[11]gmx editconf -f confout_dimer_clusteranalysis.gro -c -d 0.1 -princ -o confout_dimer_tightbox.gro

[12]gmx genconf -f confout_dimer_tightbox.gro -nbox 1 1 5 -o 10clust.gro

4.2.3.3 Using 2 molecules as a template. In Google-docs, a .gro-file was produced with 2 HPHC molecules, in a box of $8.1 \times 1.5 \times 0.6$ nm. In this box, both molecules are flat in the xy-plane, with the tail pointing in the x-direction. The nanodisc width is 1.2 nm, so with 0.3 nm between two stacks an interaction should be guaranteed[13]. The template can be repeated in the z-direction to create two π-stacks (similar to that shown in Figure 4.13b on page 25; the two nanowire-aggregates (dimer) can be repeated in the y-direction to create a membrane.

4.2.3.3.1 Small membrane (5×10). In the first attempt, a small membrane was tried. The membrane consisted of nanowires of 10 molecules long (3.7 nm), it was 5 nanowire aggregates wide (7.5 nm). The membrane fell apart because the π-stacks were too short; there was too little side-interaction.

4.2.3.3.2 Bigger membrane (10×50). In the second attempt, a bigger membrane was simulated, now the nanowires are 50 molecules long, and the membrane is 10 nanowires wide[14]. This membrane contains 1000 HPHC molecules.

Even though the structure was energy minimized, a lot of energy was released during MD simulation. The solvent started to boil, which eventually crashed the simulation. The output file was simulated, again in a new solvent box. This started to boil again. The solution found was to increase the pressure to 100 bar in the `md.mdp` file. Thanks to the pressure, simulations were running stable. The additional pressure is not elegant, but it worked for the time being, which allowed to continue work on the nanotubes. In Appendix D.1 on page 42, attempts were done to resolve the pressure problem.

4.2.4 Self-assembly step 4: Nanotubes

Membrane bending is the first step in creating a nanotube. If the membrane of any size can be bent, it should be possible create a nanotube of a certain size.

4.2.4.1 Spontaneous. If the membrane would need to bend spontaneously from a symmetrical starting situation, molecules would have to do a flip-flop to in order to increase the area of the outer layer and decrease the area of the inner layer.

The membrane formed in paragraph 4.2.3.3.2 was simulated for 1.5 μs to see whether it would bend on its own. One strand of molecules nearly moved from the top layer to the side, to form a round edge, similar to the tetramer conformation as shown in Figure 4.14 on the previous page. If this strand would have moved to the other side, the structure may have curled up into a vesicle. Unfortunately it was pushed back by a periodic image of the bilayer. This time, the solvent became compressed due to the high pressure.

But even if the vesicle would have formed in the above experiment, it would have had the nanowires along the long axis of the vesicle, unlike the literature example in which the nanowires spiralled has a helix, see Figure 4.16 or the literature [Hil+04].

---

[13]The file `HPHC_single_mem.gro` can be downloaded in Appendix A.2 on page 36

[14]The command used is: `gmx genconf -f HPHC_single_mem.gro -nbox 1 10 50 -o HPHC_membrane.gro`
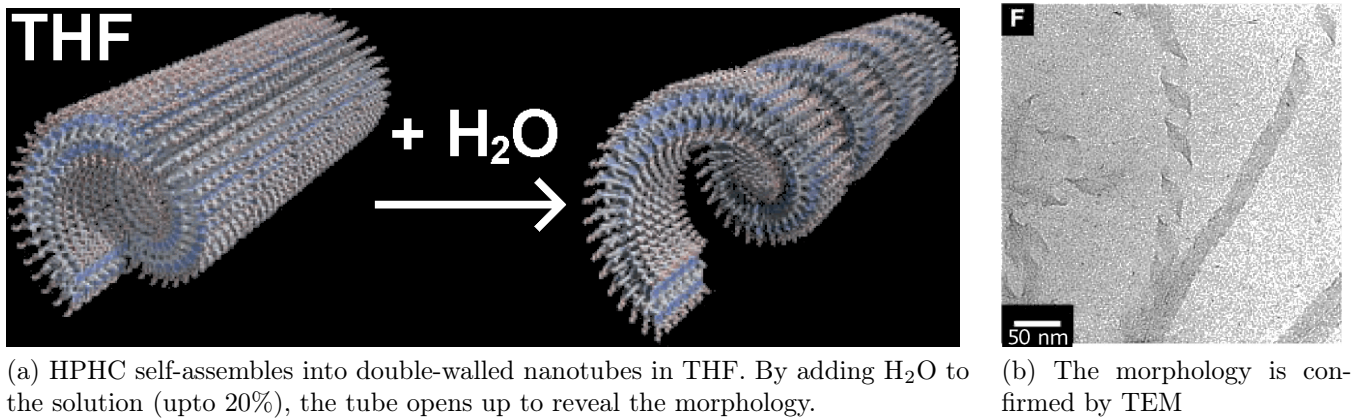
(a) HPHC self-assembles into double-walled nanotubes in THF. By adding H_2O to the solution (upto 20%), the tube opens up to reveal the morphology.

(b) The morphology is confirmed by TEM

Figure 4.16: Reprint of 2.5 on page 12. The vesicle of the literature. (a) schematic, (b) measured. Source: [Hil+04]

Note that in Figure 4.16, there are as many molecules in the inner membrane as in the outer membrane. This would mean that the area per lipid is bigger on the outside than on the inside. This is debatable and probably just a drawing error.

If molecules would need to unbalance the starting situation by doing a flip-flop in the correct manner, the $\pi - \pi$-interaction would need to be broken. This may happen at higher temperatures, but it is more likely that self-assembly never yields a symmetrical membrane.

Let's conclude that this membrane needs more help in order to bend in the proper direction.

4.2.4.2   With a little help.   The only way to bend a membrane is by making the number of lipids unequal on both sides of the membrane. vesicle would form spontaneously is if the upper and lower membrane have unequal number of HPHC molecules in it.

4.2.4.2.1   Removing molecules.   Fortunately, the membrane made in paragraph 4.2.3.3.2 on the preceding page has all molecules numbered in a nice order: because there were 2 molecules in the conformation on either side of the membrane, the HPHC_membrane_in_THF.gro-file has all molecules with an odd number[15] on one side of the membrane, and all molecules with an even number[16] on the other side of the membrane.

A script was written that would grep 9 out of 10 HPHC molecules[17]. The number of molecules that form the inner:outer leaflet is 400:500, i.e. a ratio of 4:5.

This unbalanced starting conformation was energy minimized and simulated at 100 bar[18]. After 0.1 μs, the membrane appears to have bent, see Figure 4.17 on the next page.

[15]written in the HPHC_membrane_in_THF.gro file as: 1HPHC, 3HPHC, 5HPHC, 7HPHC, 9HPHC, etc

[16]written in the HPHC_membrane_in_THF.gro file as: 2HPHC, 4HPHC, 6HPHC, 8HPHC, 10HPHC, etc

[17]One in 5 of the molecules that was on the even-numbered side of the membrane was removed.

[18]The 100 bar was added because THF was boiling at 1 atmosphere. Other pressures weren't tried.
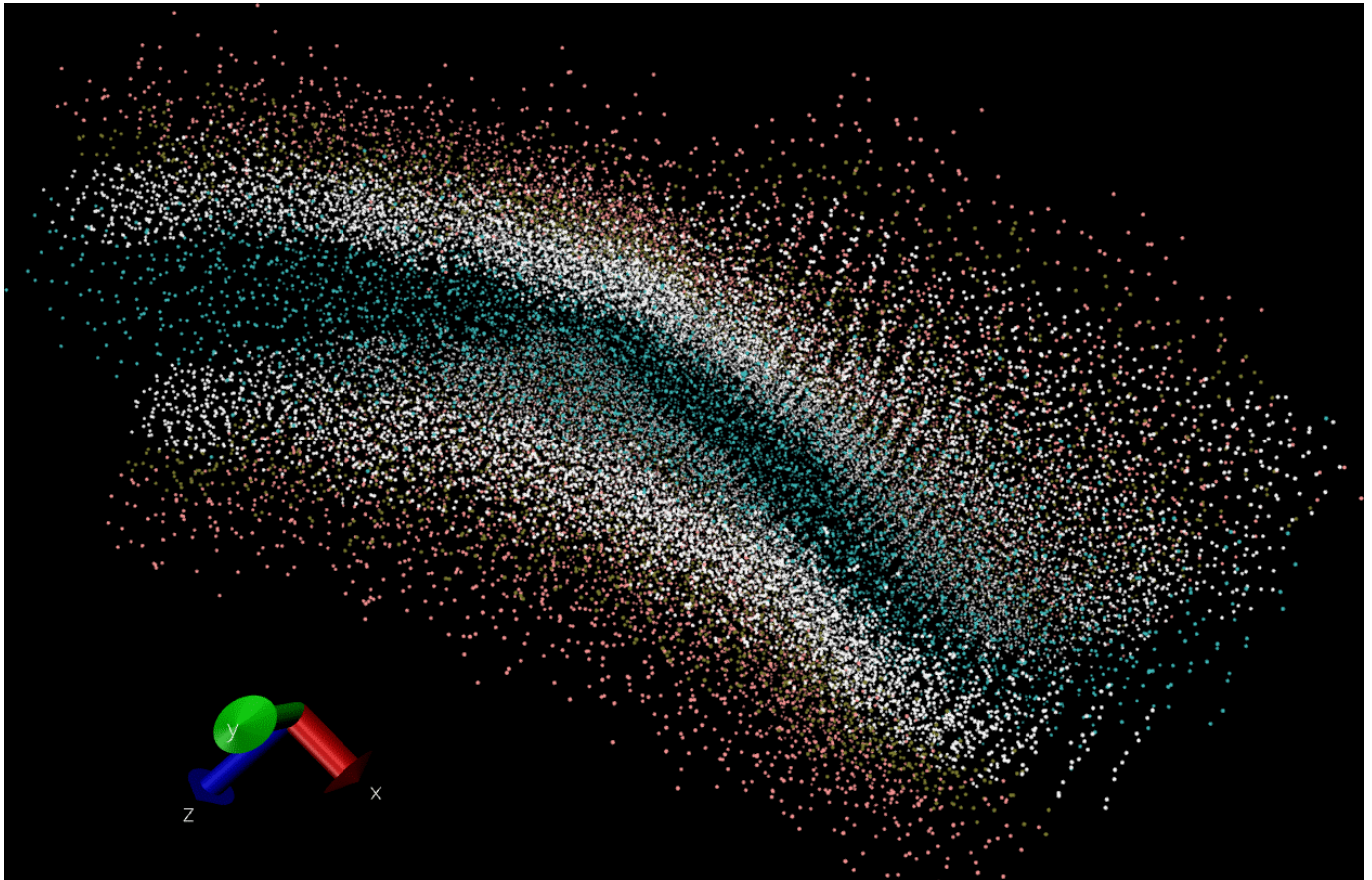
(a) The bend membrane shown in the xz plane. The curvature is best visible in this view. The curvature is approximately 35°, or one fifth of a circle, meaning that a bigger membrane is required for creating a closed
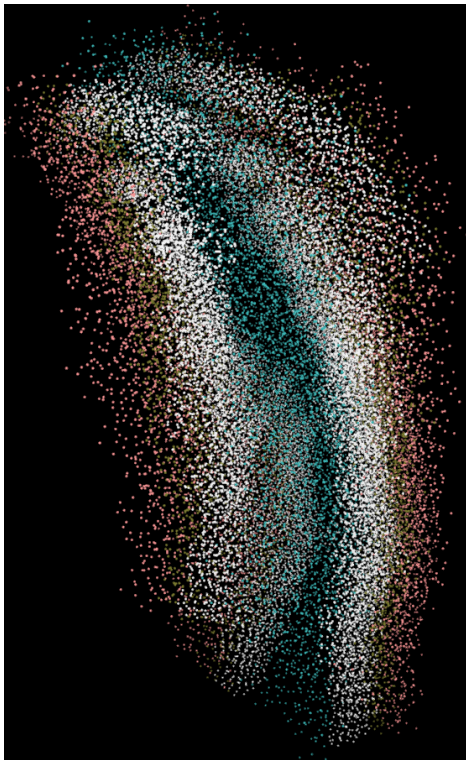
(b) The bend membrane, seen from another angle
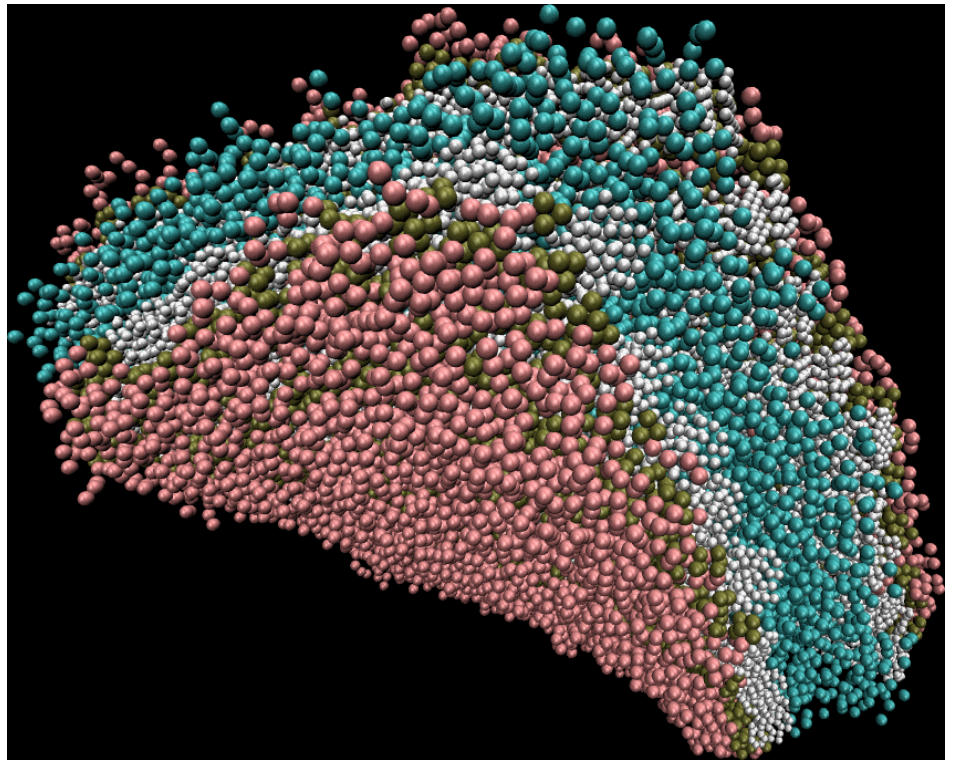
(c) VDW-drawing method gives an impression of the size of the membrane.

Figure 4.17: Membrane bending

4.2.4.2.2   How far can we go?   This slight bend is a little subtle. In an attempt to bend this membrane even further, a new script was written, see Appendix A.2 on page 36. This time the script is runs, the script sorts the molecules on whether they are on the inner or outer leaflet. This is done by first grepping all molecules that have an odd number. Next, 100 molecules are deleted. This should in principle give the same result as before, the only difference is that the .gro file contains all molecules in order, which enables us to repeat the second step (delete the first 100 HPHC molecules encountered in the .gro file), in order to delete more molecules from the same leaflet. This could in principle lead to stronger bending of the molecule, but the it remains the question whether it is realistic.

The starting conformation was troublesome, THF was boiling again at 1 atmosphere, but this time an attempt was done to fix the problem in a more elegant way: by switching off the pressure coupling, the simulation box will not expand anymore. In Appendix D.1 on page 42, the latest experiments with alternative thermo- and pressure-coupling are elaborated.

4.2.4.2.3   What is realistic?   In Figure 4.16b on page 28, the nanotube is shown in real life. According to the scale, the tube is 26 nm wide, and a complete turn of the helix is 56 nm long. If we assume that the space between 2 HPHC molecules in a π-stack is 0.37 nm, and the distance between the aromatic cores of the inner/outer leaflet is 4 nm, it can be calculated that there are 202 molecules in the inner leaflet and 236 molecules in the outer leaflet. The ratio of molecules in the inner:outer leaflet is 6:7 in the literature, while in the computer experiment a ratio of 4:5 was used. This means that it is not realistic to simulate a system in which the ratio between inner:outer leaflet is 3:5.

5 Conclusion and Further Outlook

In this bachelor thesis, the limits of CG Martini 3 were explored. In 2004, a high impact article was published on the self-assembly of Hexa-peri-hexabenzocoronene (HPHC); it forms a double-walled nanotube that unravels to a helix when water is added. The self-assembly process of this literature example was studied by MD simulation.

The HPHC model was validated before self-assembly was studied. The final model is stable with a time-step of 10 fs.

Twenty loose HPHC molecules successfully self-assembled into a nanowire, in which the $\pi - \pi$-stacking-distance is equal to the literature value for benzene.

Two nanowires successfully self-assembled into a dimer nanowire aggregate, and two dimers self-assembled into a tetramer.

A HPHC membrane was build with `gmx genconf`, it is stable and membrane bending has proven to be possible. Though the double-walled nanotube didn't form completely, the results look promising.

5.1 Further Outlook

This project. The models for coronene and hexabenzocoronene cause a bottle-neck in the stability of the CG models. Riccardo Alessandri has more experience in modelling polyaromatic compounds, he already created and validated models for naphthalene and pyrene in CG Martini, which are stable with a timestep of 40 fs, by using a brilliant combination of constraints and virtual sites. According to Riccardo, better models for coronene and hexabenzocoronene are challenging but probably possible.

When the bottlenecks in the CG models of coronene and hexabenzocoronene are resolved, MD simulations require less computational effort. This is interesting for up-scaling the simulation to the level at which complete double-walled nanotube is formed.

Next projects. In this thesis, the self-assembly process of an aromatic amphiphile was studied with `CG Martini 3`. Next projects include self-assembly processes of other aromatic amphiphiles, e.g. C_8S_3 and other cyanine dyes. According to Ilias Patmanidis, there is a lot to discover in this field.

CG Martini 3. For as far this bachelor-thesis is concerned, `Martini 3` is looking good! It was not possible to study $\pi - \pi$ stacking with `CG Martini` before! These new flavors will surely come in useful in the Martini bead-arsenal. Looking forward to the release from Paulo.

Acknowledgements

I want to thank all members of the MD group for the great experience you gave me. This motivates me even further to go for a PhD and get into a research group.

Siewert-Jan Marrink, you are a great leader for the Molecular Dynamics group in Groningen. Thank you for bringing your lovely kids to the multi-group-outing, we had loads of fun there;), and thanks for having me at the BBQ at your place.

Alex H. de Vries, thank you for doing more than just daily supervision. Thank you for helping me out of so many technical problems and thank you for all your time and effort and helpful ideas, the `clusterAnalysis.sh` script, and the non-alcoholic Martini-mix-drinks during the BBQ.

Carsten, thank you for adding me to the MD WhatsApp-group.

Antara, Bart, Carsten, Liu Yang and Sebastian, thank you for organizing the lab-uitje.

Hanif Khan, although you already left, I want to thank you for your tip's and tricks with the Linux-terminal.

Ilias Patmanidis, thank you for your help in modeling HPHC. Thank you for checking this report on typos. I wish you loads of luck with C_8S_3, I hope Martini 3 will work for you too.

Riccardo Alessandri, thank you for making and validating the THF solvent, this saved me loads of time. Thank you for showing me your inspiring models for the polyaromatic rings, your solutions are so clever!

Tsjerk Wassenaar, thank you for your effort in modifying `INSANE`.

Paulo Telles de Souza, thank you for developing Martini 3.

References

[BSD95]   H.J.C. Berendsen, D. van der Spoel, and R. van Drunen. "GROMACS: A message-passing parallel molecular dynamics implementation". In: *Computer Physics Communications* 91.1 (1995), pp. 43–56. ISSN: 0010-4655. DOI: `http://dx.doi.org/10.1016/0010-4655(95)00042-E`. URL: `http://www.sciencedirect.com/science/article/pii/001046559500042E`.

[HDS96]   William Humphrey, Andrew Dalke, and Klaus Schulten. "VMD – Visual Molecular Dynamics". In: *Journal of Molecular Graphics* 14 (1996), pp. 33–38.

[Ber+02]   H. von Berlepsch et al. "Surfactant-Induced Separation of Stacked J-Aggregates. Cryo-Transmission Electron Microscopy Studies Reveal Bilayer Ribbons". In: *Langmuir* 18.7 (2002), pp. 2901–2907. DOI: `10.1021/la011602e`. eprint: `http://dx.doi.org/10.1021/la011602e`. URL: `http://dx.doi.org/10.1021/la011602e`.

[Gre02]   Friedrich Grein. "Twist Angles and Rotational Energy Barriers of Biphenyl and Substituted Biphenyls". In: *The Journal of Physical Chemistry A* 106.15 (2002), pp. 3823–3827. DOI: `10.1021/jp0122124`. eprint: `http://dx.doi.org/10.1021/jp0122124`. URL: `http://dx.doi.org/10.1021/jp0122124`.

[Hil+04]   Jonathan P. Hill et al. "Self-Assembled Hexa-peri-hexabenzocoronene Graphitic Nanotube". In: *Science* 304.5676 (2004), pp. 1481–1483. ISSN: 0036-8075. DOI: `10.1126/science.1097789`. eprint: `https://www.orgchem.science.ru.nl/rowan/Coll/caput-college/aida.pdf`. URL: `https://www.researchgate.net/publication/8527689_Self-Assembled_Hexa-peri-hexabenzocoronene_Graphitic_Nanotube`.

[MVM04]   Siewert J. Marrink, Alex H. de Vries, and Alan E. Mark. "Coarse Grained Model for Semiquantitative Lipid Simulations". In: *The Journal of Physical Chemistry B* 108.2 (2004), pp. 750–760. DOI: `10.1021/jp036508g`. eprint: `http://dx.doi.org/10.1021/jp036508g`. URL: `http://dx.doi.org/10.1021/jp036508g`.

[KD06]   Stefan Kirstein and Siegfried Daehne. "J-Aggregates of Amphiphilic Cyanine Dyes: Self-Organization of Artificial Light Harvesting Complexes". In: *International Journal of Photoenergy* 2006.(???) (2006). Article ID 20363, pp. 1–21. DOI: `10.1155/IJP/2006/20363`. eprint: `https://www.hindawi.com/journals/ijp/2006/020363/abs/`. URL: `http://dx.doi.org/10.1155/IJP/2006/20363`.

[Mar+07]   Siewert J. Marrink et al. "The MARTINI Force Field: Coarse Grained Model for Biomolecular Simulations". In: *The Journal of Physical Chemistry B* 111.27 (2007). PMID: 17569554, pp. 7812–7824. DOI: `10.1021/jp071097f`. URL: `http://dx.doi.org/10.1021/jp071097f`.

[HLG11]   Wei Huang, Zhixiong Lin, and Wilfred F. van Gunsteren. "Validation of the GROMOS 54A7 Force Field with Respect to β-Peptide Folding". In: *Journal of Chemical Theory and Computation* 7.5 (2011). PMID: 26610119, pp. 1237–1243. DOI: `10.1021/ct100747y`. eprint: `http://dx.doi.org/10.1021/ct100747y`. URL: `http://dx.doi.org/10.1021/ct100747y`.

[Mal+11]   Alpeshkumar K. Malde et al. "An Automated Force Field Topology Builder (ATB) and Repository: Version 1.0". In: *Journal of Chemical Theory and Computation* 7.12 (2011). PMID: 26598349, pp. 4026–4037. DOI: `10.1021/ct200196m`. eprint: `http://dx.doi.org/10.1021/ct200196m`. URL: `http://dx.doi.org/10.1021/ct200196m`.

[MT13]   Siewert J. Marrink and D. Peter Tieleman. "Perspective on the Martini model". In: *Chem. Soc. Rev.* 42 (16 2013), pp. 6801–6822. DOI: `10.1039/C3CS60093A`. URL: `http://dx.doi.org/10.1039/C3CS60093A`.

[PM13] Xavier Periole and Siewert-Jan Marrink. "The Martini Coarse-Grained Force Field". In: Humana Press, 2013, pp. 533–565. DOI: `10.1007/978-1-62703-017-5_20`. URL: `https://www.researchgate.net/publication/232010032_The_Martini_Coarse-Grained_Force_Field`.

[Abr+15] Mark James Abraham et al. "GROMACS: High performance molecular simulations through multi-level parallelism from laptops to supercomputers". In: *SoftwareX* 1–2 (2015), pp. 19–25. ISSN: 2352-7110. DOI: `https://doi.org/10.1016/j.softx.2015.06.001`. URL: `http://www.sciencedirect.com/science/article/pii/S2352711015000059`.

[Was+15] Tsjerk A. Wassenaar et al. "Computational Lipidomics with insane: A Versatile Tool for Generating Custom Membranes for Molecular Simulations". In: *Journal of Chemical Theory and Computation* 11.5 (2015). PMID: 26574417, pp. 2144–2155. DOI: `10.1021/acs.jctc.5b00209`. eprint: `http://dx.doi.org/10.1021/acs.jctc.5b00209`. URL: `http://dx.doi.org/10.1021/acs.jctc.5b00209`.

Including unpublished work of:

Paulo Telles de Souza: Martini 3, 2017.

Appendices

A Scripts

A.1 Validation

If the coarse-grained-bead numbers are written under "cgnr." in the `AA.itp` file, `Mapbuilder.sh` will be able to grep it and create a indexfile that you can use to map your trajectory from all atom (AA) to coarse grained (CG), so that it can be easily used for analysis.

Example of an `AA.itp` file:
https://www.dropbox.com/s/qedboatjobk7xns/Octylbenzene_AA_for_CG.itp?dl=0

`Mapbuilder.sh`: https://www.dropbox.com/s/ke43m2ayey94tmj/mapbuilder.sh?dl=0

Once the indexfile "`AA_to_CG_map.ndx`" is made, the AA-trajectory can converted to a coarse-grained trajectory by using the "`convert_AA_traj_to_CG.sh`" script. This script is so super easy that it is actually possible to just show it in text:

```bash
#!/bin/bash
beadspermol=5
nmols=20      # Number of molecules
numberofgroups=$(($nmols*$beadspermol))
AAtrajname="AA/traj_comp.xtc"
seq 0 $(($numberofgroups-1)) | gmx traj -f $AAtrajname -s AA/topol.tpr -oxt
traj_AA_mapped_as_CG.gro -n AA/AA_to_CG_map_simple.ndx -com -ng $numberofgroups -b 1000
```

`convert_AA_traj_to_CG.sh`: https://www.dropbox.com/s/khetsvua7uxn3kk/convert_AA_traj_to_CG.sh?dl=0

For the `CG.itp` for which you want to optimize bonded parameters, I wrote a script that can grep useful bonded names from the the comments. The script does need a little help: you need to make the end of the bead-line visible by changing function 1 to 1f as follows:

```
[angles]
   ; i   j    k   funct   angle   force.c.
    1    2    4    1f      150     500     ; perspective 1
    1    2    6    1f       90     500     ; square 1
    1    5    6    1f       90     500     ; square 1
    1    5    7    1f      120     500     ; diamond 1
   27   28   29    1f      130      50     ; TEGtail180 on the left side of my molecule
```

Example of an `CG.itp` file: https://www.dropbox.com/s/4ljjlqv58ppjk93/Octylbenzene_CG_for_indexer.itp?dl=0

`indexer.sh`: https://www.dropbox.com/s/dup3p1sknk3wxkd/indexer.sh?dl=0

The script `indexer.sh` will grep the useful names (e.g. perspective, square, diamond, TEGtail, etc), and create an indexfile that looks like this:

[diamond]	[square]
1 5 7	1 2 6
41 45 47	41 42 46
81 85 87 ...	81 82 86 ...
[perspective]	[TEGtail180]
1 2 4	27 28 29
41 42 44	67 68 69
81 82 84 ...	107 108 109 ...

Etc. There are 40 beads in HPHC, the above indexfile point to the identical angles of 3 HPHC molecules, by moving a template by 40 lines. Bonds and dihedrals can be put here too. These indexfiles (`angles.ndx`, `bonds.ndx` and `dihedrals.ndx` can then be fed to `calc_dists.sh` script.

`calc_dists.sh`: https://www.dropbox.com/s/oxfht3k3tlnmvbc/calc_dists.sh?dl=0

It will nicely plot your distributions.

A.2   Membranes

The first bilayer-template can be downloaded here:
https://www.dropbox.com/s/0g871q3olzx6ko9/HPHC_single_mem_old.gro?dl=0

The second template is better because there is less space between the inner/outer leaflet, and because the nanodiscs are at the ideal CG-martini π-stack-distance (0.3725 nm). As a result, a membrane build from this template equilibrates faster.
https://www.dropbox.com/s/44yoohturgtlw8e/HPHC_single_mem_new.gro?dl=0

The next script (`bendscript.sh`) was written to bend the membrane.
https://www.dropbox.com/s/eh6b49mw68537wo/bendscript.sh?dl=0

The initial idea was to remove just 1 in 4 molecules from one of the leaflets, but this script is adjusted as such that it will first sort molecules (whether they are on the upper or lower membrane), and then it will remove 100 lines. Note that it also writes the topol.top file for you :)

Critical side note: it is not necessary to remove more than 1 in 5 molecules on one side of the leaflet, because the ratio between inner:outer-leaflet in the coarse-grained double-walled nanotube is 4:5, which is already more out of balance than in the real double-walled nanotube (6:7). Removing 2 molecules on one side of the leaflet would be theoretically interesting, but for now ratio between inner:outer-leaflet of 3:5 was considered to be too far from reality. It would be great if it would work, because it will increase the extend of bending of the membrane, which will allow the nanotube to be formed in a smaller box, which will reduce the required computational effort.

B   Optimized parameters for HPHC

B.1   Mapping and values

The bead numbering used is shown in Figure B.1. The inputfiles can be downloaded in B.2.1 on the next page. Below, a few lines of the `HPHC_VALIDATED_model4_softmod.itp` file are given, so that it is clear what bonds/angles/dihedrals were used on what atoms.

[bonds]

; i	j	funct	length	force.c.	name (occurance [extra info])
1	3	1	0.2674	25000	; HXB_arom_bond (34x)
1	2	1	0.2674	25000	; HXB_gap_bond (5x)
1	6	1	0.3782	25000	; HXB_diag_bond (8x)
17	24	1	0.285	25000	; phen_con_bond (4x)
15	24	1	0.4833	25000	; phen_FF (2x [Force Flat])
24	25	1	0.285	25000	; phen_arm_bond (6x [benzene bond])
25	27	1	0.285	25000	; TEG_con (4x [TEG connect])
24	27	1	0.4936	25000	; lr_TEG_FF (2x [TEG Force Flat])
27	28	1	0.330	17000	; TEG_bond (6x [Lee's model])
1	35	1	0.47	2500	; ATC (4x [Aliphatic connect])
35	36	1	0.47	2500	; ATB (4x [Aliphatic bond])

[angles]

; i	j	k	funct	angle	force.c.	name (occurance [extra info])
1	3	7	1	120	1000	; diamond (16x)
1	5	10	1	180	250	; trace (16x)
9	10	11	1	180	250	; gtrac (2x)[note A]
1	2	6	1	90	500	; square (5x)[note B]
1	2	4	1	150	500	; perspective (4x)[note C]
15	24	27	1	180	80	; bisphenFF (2x)
24	25	27	2	120	50	; PhDiamond (4x)
24	27	28	1	180	15	; PhTEG (2x)
27	28	29	1	130	50	; TEGtail (4x)
5	35	36	2	180	25	; PhAT AliFF2 (2x)
35	36	37	2	180	25	; Alistr (2x [dodecane])

note A: gtrac is a trace angle that jumps over the hexabenzocoronene gap. It has a different label in order to measure it separately.

note B: The first square (atoms 1, 2, 6, 5) was modeled with 2 square angles, but the other squares got modeled with 1 square angle.

note C: The "perspective" angle ensures a non-flexible edge.

[dihedrals]

; i	j	k	l	funct	angle	force.c.	mult	name (occurance [extra info])
22	21	23	31	2	0	100		; phenylFF@bisphen (2x)
25	26	17	19	1	45	2	4	; bisphenrot (4x)
5	1	3	35	2	180	25		; aliphatic_out_of_plane (2x)
24	25	26	27	2	180	100		; phenTEG_out_of_plane (2x)
; 9	1	20	12		180			; HBC_macro1 [just measured]
; 9	5	16	12		180			; HBC_macro2 [just measured]

Note that "HBC_macro1" and "HBC_macro2" are used for measuring the stiffness of hexabenzocoronene, see Appendix C.1 on page 39.
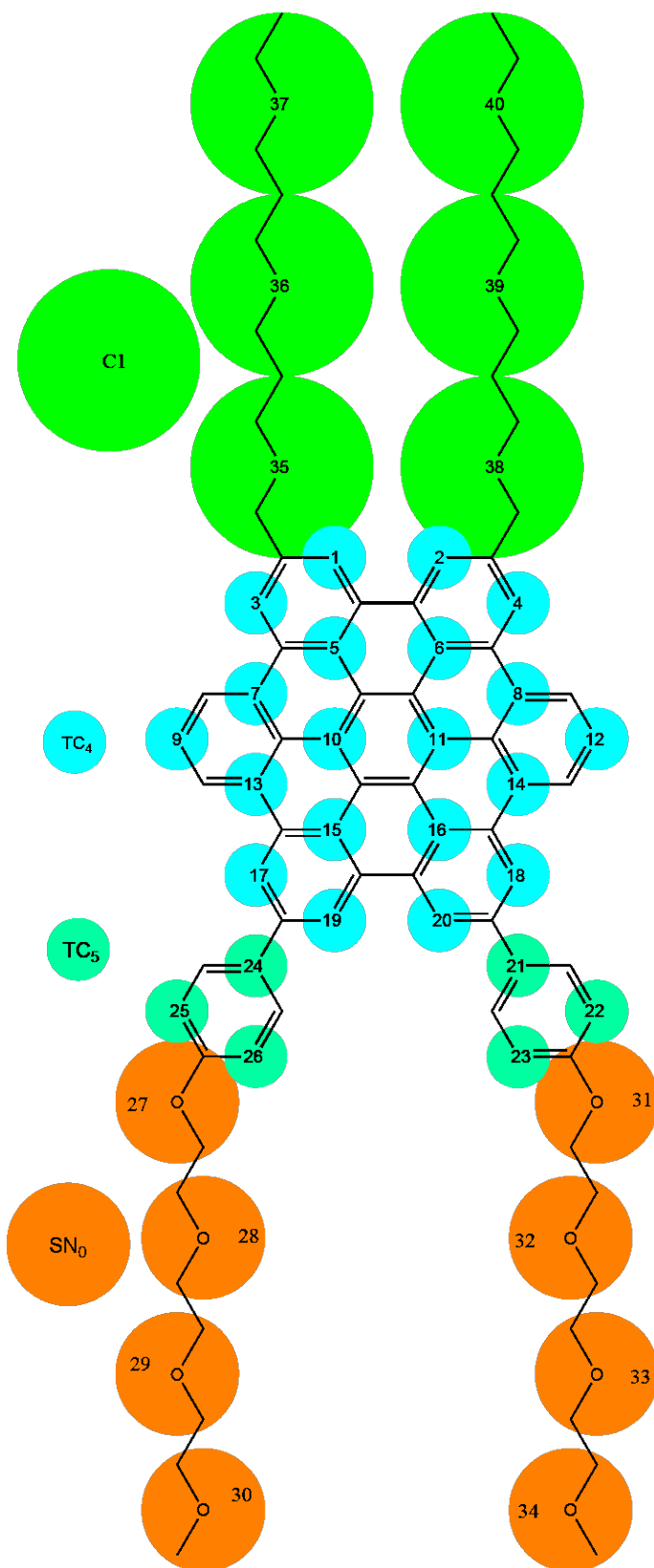

Figure B.1: The bead numbering in the HPHC molecule.

B.2   Downloads

B.2.1   HPHC CG files

The first validated hexa-peri-hexabenzocoronene (HPHC) model can be downloaded via:
`https://www.dropbox.com/s/57y1vk4ta2u3lqo/HPHC_VALIDATED_model2.itp?dl=0`

The second validated HPHC model contains softer angles and more bonds.
`https://www.dropbox.com/s/4kpaf7382j41pte/HPHC_VALIDATED_model4.itp?dl=0`

The constraint network (Figure 4.5c on page 18) was included in model 5, but it wasn't stable in big systems (links-errors).
`https://www.dropbox.com/s/8zld5bqcu0efwc5/HPHC_VALIDATED_model5.itp?dl=0`

When building membranes, even the two constraints to connect the TEG-tail became trouble-some, so they were replaced by bonds as well.
`https://www.dropbox.com/s/7v7xk9oycf2la01/HPHC_VALIDATED_model4_softmod.itp?dl=0`

The latest model of hexa-peri-hexabenzocoronene, developed in Appendix D.2 on page 43, is expected to work with a time-step of 20 fs too, it also makes use of the long bonds proposed in Figure 4.5c on page 18, but then it uses bonds instead of constraints. The hexabenzocoronene (HBC)-model runs stable! The new HPHC model was tested on Monday 4th of September, with success!
`https://www.dropbox.com/s/hqkxzyz71kvjuez/HPHC_VALIDATED_model5.itp?dl=0`

B.2.2   All Atom (AA) files from the ATB server

Hexa-peri-hexabenzocoronene: `https://atb.uq.edu.au/molecule.py?molid=151365`

Hexabenzocoronene: `https://atb.uq.edu.au/molecule.py?molid=108519`

Coronene: `https://atb.uq.edu.au/molecule.py?molid=29903`

Octylbenzene: `https://atb.uq.edu.au/molecule.py?molid=21087`

TEG-tail connected to a benzene ring: `https://atb.uq.edu.au/molecule.py?molid=119921`

Bisphenyl link between HBC and TEG: `https://atb.uq.edu.au/molecule.py?molid=108457`

C Validation - Results & Discussion

In the previous section, the validated bonded parameters were given. The intention of this section is to provide distributions for some parameters measured or defined.

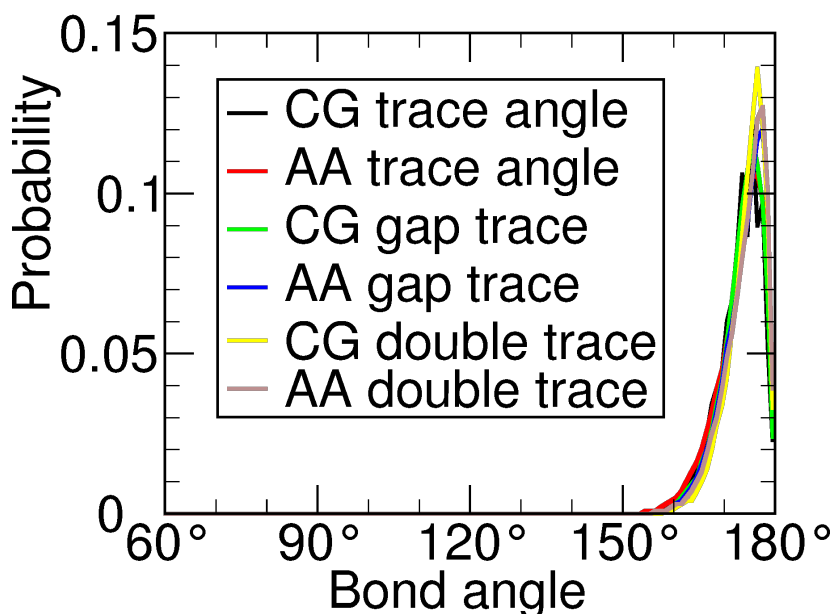## C.1 Stiffness of Hexabenzocoronene (HBC)

There were no dihedrals used in modeling the aromatic hexabenzocoronene (HBC) core. Instead, there was a network of strong angles that made sure that HBC was flat. To see whether the stiffness was good, three straight angles (see Figure C.1a) and two dihedrals (see Figure C.2a and Figure C.2b) were measured.

According to Figure C.1b, all angles have approximately the same distribution. This is great, because it means that the all atom-model is just as stiff as the coarse-grained model. Critical side note, however: most angles measured (trace and gap trace) are also defined, so the double trace angle is the only angle which is measured without an explicit force on it. It is better to measure stiffness via a dihedral.
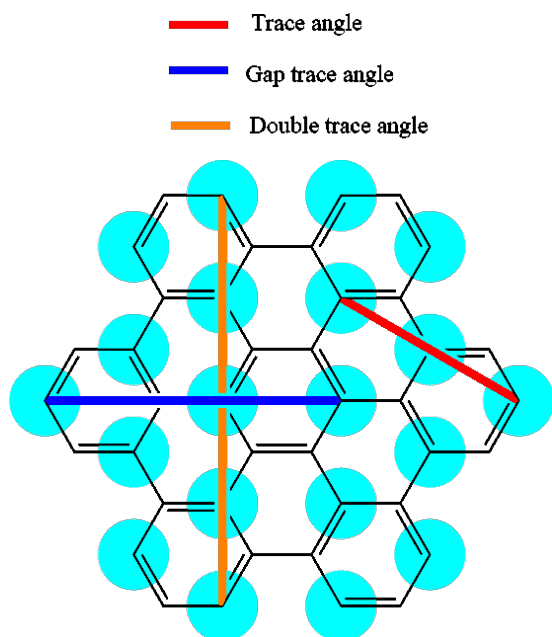
(a) Definition of the measured angles. "Trace" in **red**, "Gap trace" in **blue**, "Double trace" in **orange**.
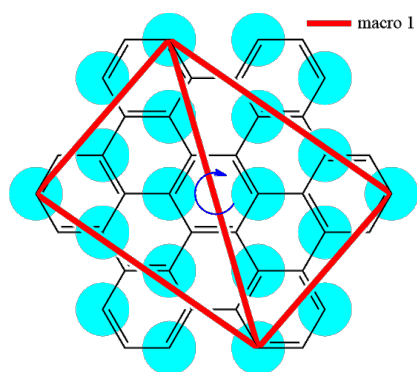
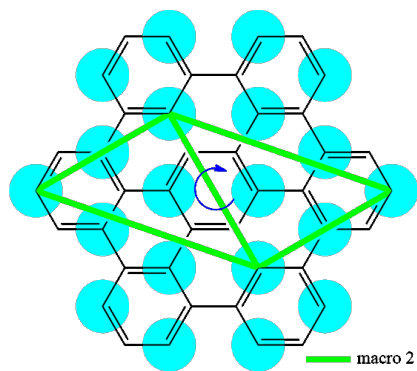(b) HBC stiffness angle distribution.

Figure C.1: The stiffness of hexabenzocoronene (HBC), measured via angles.
The distributions of the coarse grained (CG) and all atom (AA) models overlap, meaning that the CG model is just as stiff as the AA model.

In Figure C.2c on the next page, the black line is underneath the blue and the green line. This means that the CG model of hexabenzocoronene is slightly stiffer than the AA model.
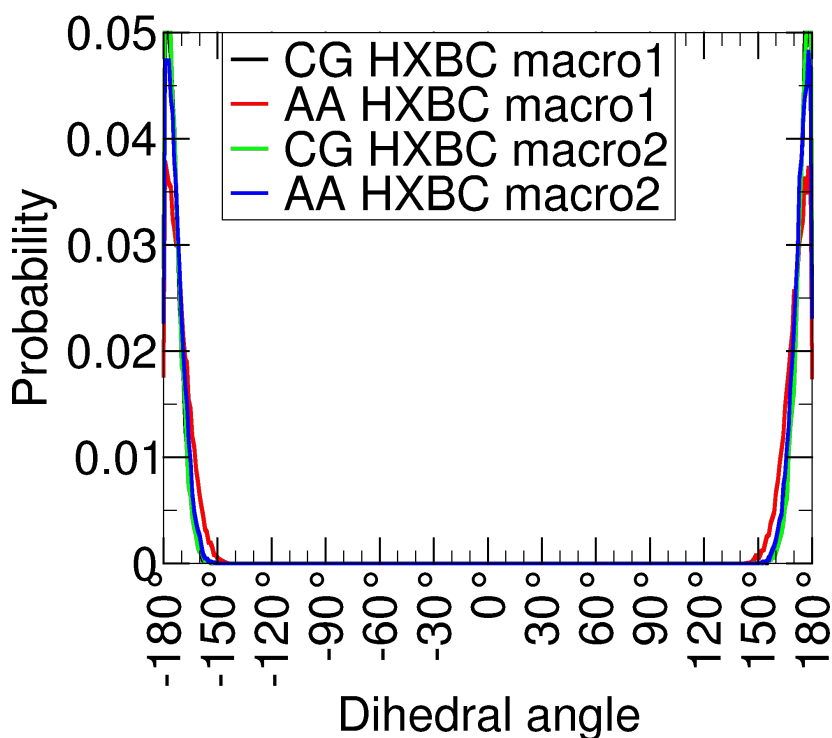
(a) Dihedral "Macro1"

(b) Dihedral "Macro2"


Distribution of dihedral angles

(c) HPHC stiffness dihedral distributions

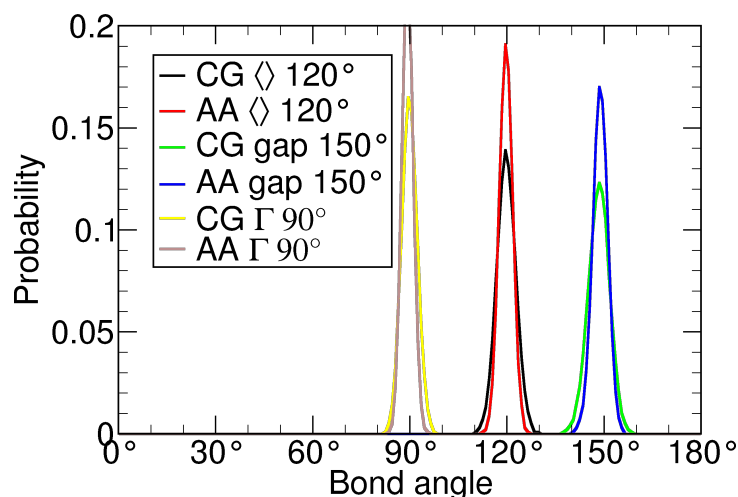Figure C.2: The stiffness of hexabenzocoronene (HBC), measured via dihedrals.
Note that the black line is under the blue and the green line.
The distributions of the coarse grained (CG) and all atom (AA) models for macro2, but for macro1, the CG model (black) displays a sharper distribution than the AA model (red), meaning that the CG model is slightly stiffer than the AA model.
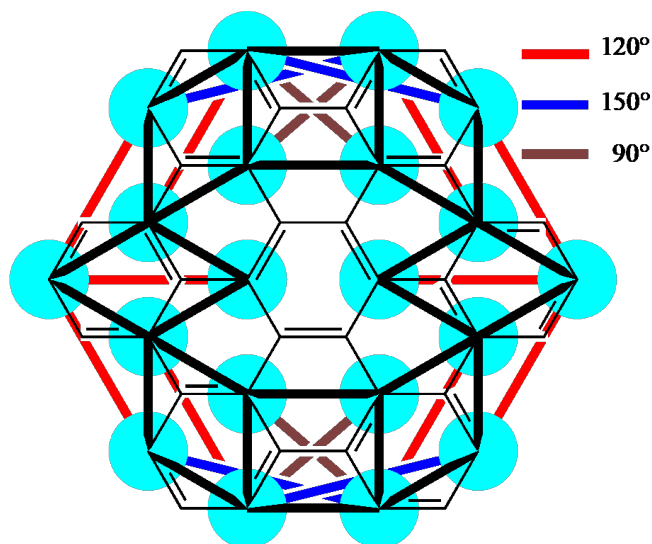
(a) Definition of the measured aromatic angles. "Diamond" in **red**, "Perspective" in **blue**, "Square" in **brown**.

Distribution of aromatic angles

(b) HBC aromatic angle distribution.

Figure C.3: The hexabenzocoronene (HBC) is primarily defined by it's aromatic angles.
Note that the aromatic angles are used to provide local stiffness on the edge of the nanodisc. The fact that the distributions of the coarse grained (CG) and all atom (AA) models overlap, does not mean anything here.
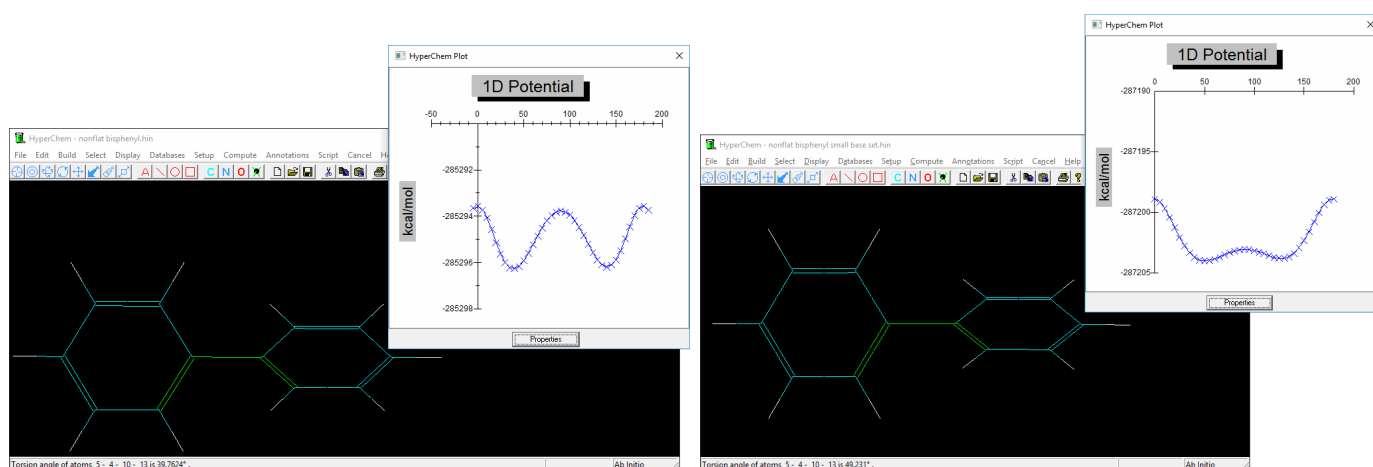
C.2   Bisphenyl dihedral

One interesting dihedral is the dihedral between the two phenyl rings, they prefer to be at 45° from each other, see Figure C.4d.

In order to check whether the all atom model was reasonable, the potential of the dihedral was also calculated with a quantum calculation in `HYPERCHEM`, see the other Figures in C.4.

The optimum dihedral of 45° was in good agreement with the dihedral potential calculated with the minimal base set, see Figure C.4a.

When the base-set was increased, however, the π-cloud becomes increasingly polarizable, and the conformation of 90°becomes less unfavourable because the electron cloud can be polarized, i.e. electrons on the hydrogen are now able to pushed the π-cloud away, see Figures C.4b and C.4c.
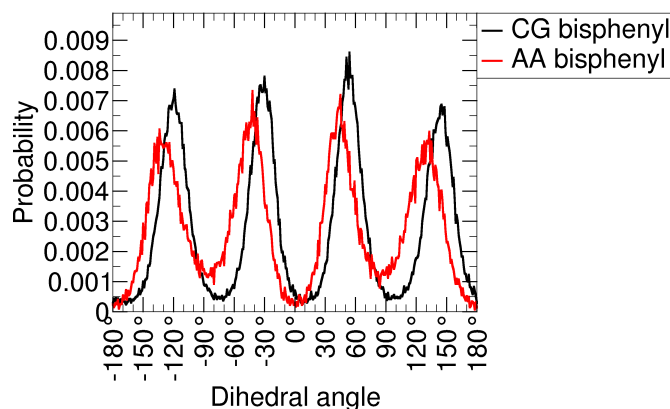

(a) Quantum calculation, minimal base set (STO-3G).

(b) Quantum calculation, small base set (3-21G).
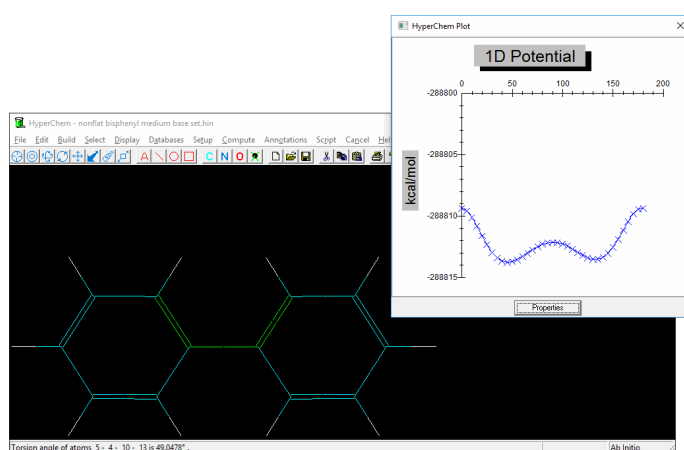
(c) Quantum calculation, medium base set (6-31G*).

(d) Bisphenyl angle distribution with the AA-model of the ATB server (B3LYP/6-31G*), and the CG-Martini model as used.

Figure C.4: Computations on the bisphenyl dihedral angle. (a, b, c), quantum calculations using HF in HyperChem. (d)

The computational experiment is consistent with literature[Gre02]. It was concluded that the bisphenyl dihedral angle can be accepted.

D Late discoveries

Some discoveries came late, e.g. new `.mdp`-settings, new CG models for HPHC. Unfortunately, there was no time to redo all simulations with the new settings. In this chapter, the latest discoveries are shown.

D.1 Pressure problem.

As mentioned in paragraph 4.2.3.3.2 on page 27, the starting structure was not relaxed, and caused solvent to boil. The idea was to fix the box-size by changing the `Pcoupl` from `Berendsen` to `None`. However, `parrinello-rahman` was used as `Pcoupl` and `Berendsen` as `tcoupl`. By mistake, the `tcoupl` was changed from `Berendsen` to `None`. This system was simulated for 1 nanosecond (dt = 5 fs). The first 25 picoseconds, the box decreased in size, and the membrane started to bend. `gmx energy -f ener.edr` showed that the temperature was very stable at 217K. This explained why THF wasn't boiling anymore and why the unit cell shrunk. The shrinking unit-cell helped the membrane bend.

Table 2: The temperature of the simulation without thermostat. (`tcoupl` = `None`)

Energy	Average	Err.Est.	RMSD	Tot-Drift	
Temperature	217.704	2.6	17.3557	15.9706	(K)

So, after 1 nanosecond, the membrane is bent (thermostat = No, dt = 5 fs).

When the thermostat was switched on again, the temperature increases to 320K and the unit cell expands. Thanks to the `Pcoupltype = isotropic`, the unit cell expands equally in all directions, so also in the bending-direction. Because the $\pi - \pi$ is so much stronger than the tail-tail interaction, the molecules start to migrate, and the membrane bends back to flat again, as shown in Figure D.1.
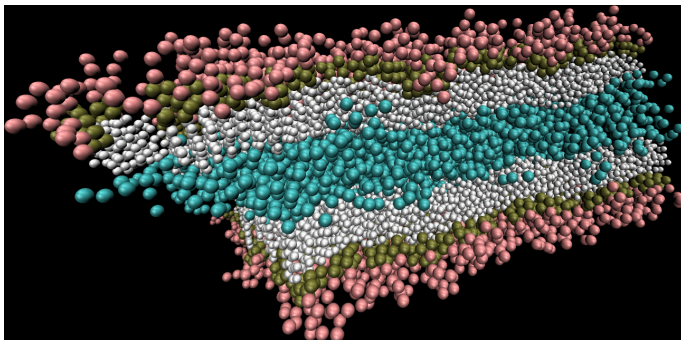

Figure D.1: The HPHC membrane bends back when the unit cell expands.

Table 3: The temperature when the thermostat switched back on again (`tcoupl` = `Berendsen`).

Energy	Average	Err.Est.	RMSD	Tot-Drift	
Temperature	319.867	0.035	2.53645	0.203314	(K)

The snapshots shown in Figure 4.17 on page 29 are still under 100 bar. In an attempt to resolve the pressure problem, all constraints were removed from the HPHC model. After that, the template was energy minimized before the membrane was built.

Though this turned out to be the way to go, it was already clear from Figure 4.17 that a bigger membrane had to be build before the double walled nanotube would be formed.

Bigger membranes require more computational effort, meaning that this the moment to revisit the coarse grained HPHC model, and hopefully create a model that runs stable with greater time-steps.

D.2   Elaborating on the hexabenzocoronene model.

As mentioned in paragraph 4.1.2 on page 18, there are many ways to define coarse grained models for hexabenzocoronene.

(a) Angle network   (b) Bonded network   (c) 'Long bonds' tested for constraints
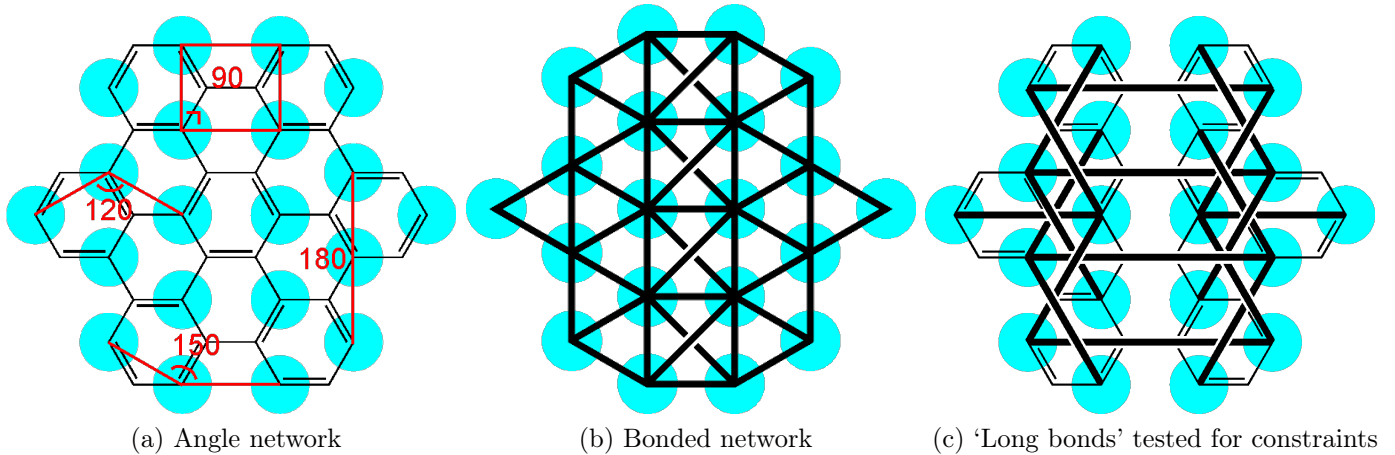
Figure D.2: Various definitions of bonds and angles in hexabenzocoronene. Together, this combination of parameters ensure that hexabenzocoronene is flat and stable. Reprint of Figure 4.5 on page 18.

When the 'long bonds' are included in the model, the spring-constant of the diamond angles could be reduced, creating more stable simulations. They appeared stable as constraints but when this HBC model was applied in the HPHC model, simulations crashed due to links-erros. It was then concluded that constraints are not robust enough for this system.

On the last working day, the HBC model was revisited, this yielded a new version of the HBC model. Here, the same 'long bonds' as above, are defined as bonds with a spring-constant of 15000. It runs stable with dt = 20 fs.
Hexabenzocoronene.itp: `https://www.dropbox.com/s/e5ai337ged3svpu/HBHC_CG_model7_softmod_concept.itp?dl=0`

Note that `md.mdp` settings were also changed here: Berendsen is both used as a thermostat (thermocoupling) and for pressure-coupling.

md.mdp: `https://www.dropbox.com/s/5p84p2g96xpm5ay/md_dt=20fs.mdp?dl=0`

The new HBC model was applied to the HPHC model and tested on Monday 4th of September. It works! :)

Download the latest version of HPHC here:

HPHC_CG.itp: `https://www.dropbox.com/s/hqkxzyz71kvjuez/HPHC_VALIDATED_model5.itp?dl=0`

D.3 Membrane bending: Level up!

Armed with the new HPHC model, new attempts to produce a double walled nanotube seem feasible, so they are tried next. The membrane needs to be 5 times as long as the one tried in section 4.2.3.3.2 on page 27. In order to reduce computational effort, attempts are done to make use of the periodic boundary condition. In order to do so, the membrane template was rotated and energy minimized to the new HPHC model.

The new membrane template: `https://www.dropbox.com/s/6bxyhugvcpz3ycp/HPHC_single_mem_mod5_new.gro?dl=0`

The first attempt appeared promising, after a few moments the membrane had allready bent to a half tube, see Figure D.3a. Note that the pressure was reduced, so that that the box would shrink, or at least, that's what I hoped what would happen. Due to a lack of interaction between the THF molecules, however, THF became a gas-phase, so the box expanded, and the density became even lower. Due to a lack of THF molecules inside the double walled nanotube, the tube collapses, see Figure D.3b.

After more extensive testing, this membrane bending didn't turn out to be the

`http://rextester.com/VILPH39885`

(a) Membrane bending, half way there   (b) The pressure was reduced, so that that the box would shrink, or at least, that's what I hoped what would happen. Due to a lack of pressure of THF, however, the double walled nanotube collapsed.

Figure D.3: The latest work on membrane bending.
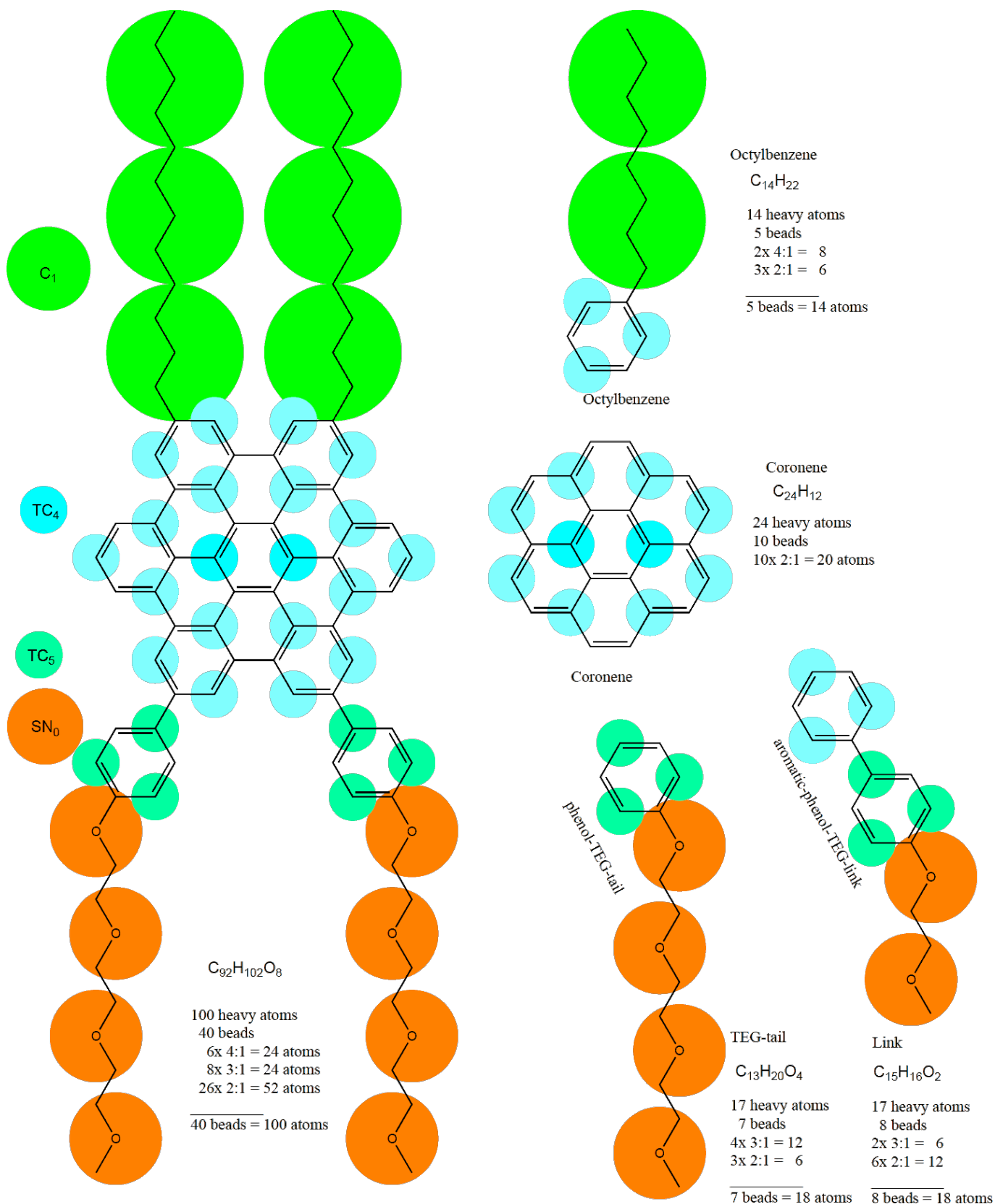
E   Model on poster format

Figure E.1: Modeling the hexa-peri-hexabenzocoronene molecule. Left: The entire molecule. Right: fragments of this molecule. Note that the center of mass of a bead is in most cases on an atom, but in the hexabenzocoronene there is an exception. This was elaborated in Figure 4.4 on page 18.